CHEMMEDCHEM

CHEMISTRY ENABLING DRUG DISCOVERY

Accepted Article

Title: Structure-based drug design of mineralocorticoid receptor antagonists to explore oxosteroid receptor selectivity

Authors: Anneli Nordqvist, Gavin O'Mahony, Maria Fridén-Saxin, Marlene Fredenwall, Anders Hogner, Kenneth L. Granberg, Anna Aagaard, Stefan Bäckström, Anders Gunnarsson, Tim Kaminski, Yafeng Xue, Anita Dellsén, Eva Hansson, Pia Hansson, Ida Ivarsson, Ulla Karlsson, Krister Bamberg, Majlis Hermansson, Jennie Georgsson, Bo Lindmark, and Karl Edman

To be cited as: *ChemMedChem* 10.1002/cmdc.201600529

Link to VoR: http://dx.doi.org/10.1002/cmdc.201600529

A Journal of

ChemPubSoc Europe

WILEY-VCH

www.chemmedchem.org

10.1002/cmdc.201600529

WILEY-VCH

FULL PAPER

Structure–based drug design of mineralocorticoid receptor antagonists to explore oxosteroid receptor selectivity

Anneli Nordqvist,*[a] Gavin O'Mahony,[a] Maria Fridén-Saxin,[a] Marlene Fredenwall,[a] Anders Hogner,[a] Kenneth L. Granberg,[a] Anna Aagaard,[b] Stefan Bäckström,[b] Anders Gunnarsson,[b] Tim Kaminski,[b] Yafeng Xue,[b] Anita Dellsén,[b] Eva Hansson,[b] Pia Hansson,[b] Ida Ivarsson,[b] Ulla Karlsson,[b] Krister Bamberg,[a] Majlis Hermansson,[a] Jennie Georgsson,[a] Bo Lindmark[a] and Karl Edman[b]

[a] Dr. A. Nordqvist, Dr. G. O'Mahony, Dr. M. Fridén-Saxin, M. Fredenwall, Dr. A. Hogner, Dr. K.L. Granberg, Dr. K. Bamberg, M. Hermansson, Dr. J. Georgsson and B. Lindmark,
Cardiovascular and Metabolic Diseases, Innovative Medicines and Early Development Biotech Unit,
AstraZeneca, Pepparedsleden 1, Mölndal, 431 83, Sweden.
E-mail: anneli.nordqvist@astrazeneca.com

[b] Dr. A. Aagaard, Dr. S. Bäckström, Dr. A. Gunnarsson, Dr. T. Kaminski, Dr. Y. Xue, A. Dellsén, E. Hansson, P. Hansson, I. Ivarsson, U. Karlsson, and Dr. K. Edman,
Discovery Sciences, Innovative Medicines and Early Development Biotech Unit,
AstraZeneca, Pepparedsleden 1, 431 83 Mölndal, Sweden.

Supporting information for this article is given via a link at the end of the document.

Abstract: The mineralocorticoid receptor (MR) is a nuclear hormone receptor involved in regulation of body fluid and electrolyte homeostasis. In this study we explore selectivity triggers for a series of non-steroidal MR antagonists to improve selectivity over other members of the oxosteroid receptor family. A biaryl sulfonamide compound was identified in a high-throughput screening (HTS) campaign. The compound bound to MR with a pK_i=6.6, but displayed poor selectivity over the glucocorticoid receptor (GR) and the progesterone receptor (PR). Following X-ray crystallography of MR in complex with the HTS hit, a compound library was designed that explored an induced fit hypothesis that required movement of the Met852 side-chain. An improvement in MR selectivity of 11–79-fold over PR and 23–234-fold over GR was obtained. Given the U-shaped binding conformation, macrocyclizations were explored yielding a macrocycle that bound to MR with a pK_i=7.3. Two protein–ligand X-ray structures were determined confirming the hypothesized binding mode for the designed compounds.

Introduction

The glucocorticoid receptor (GR), the mineralocorticoid receptor (MR), the progesterone receptor (PR) and the androgen receptor (AR) form the oxosteroid receptor family (NR3C1-4).[1] They are ligand activated transcription factors with crucial roles in a broad range of fundamental biological functions, ranging from reproduction and development to cognition and stress response. The challenge in generating subtype selective ligands lies in the fact that the steroid receptors all bind cholesterol derivatives and several structural features of the ligand binding pockets are conserved across the receptor family. Therefore, designing a selective compound requires detailed understanding of the structure–activity relationship (SAR) across the receptor family.

MR is activated by the hormone aldosterone and plays a crucial role in body fluid and electrolyte homeostasis. There are currently two MR antagonists, eplerenone and spironolactone, in clinical use for treatment of high blood pressure and heart failure.[2-5] More recently, benefits of MR blockade have been explored in chronic kidney disease (CKD) where spironolactone on top of antihypertensive medication reduced proteinuria.[7-9] However, the use of both spironolactone and eplerenone is contraindicated in diabetic patients with CKD due to the risk of hyperkalemia. In addition, the use of spironolactone is further hampered by sexual side effects that are caused by poor selectivity over AR and PR.[10] Thus, there is a great interest in the discovery and development of novel, selective MR antagonists with improved efficacies and side effect profiles to treat CKD in patients. A number of non-steroidal MR antagonists have been reported in the literature[11] of which finerenone[12] has recently completed phase II clinical trials (ARTS-HF and ARTS-DN) and Bayer AG is now conducting two phase III trials in diabetic kidney disease (FIGARO-DKD, FIDELIO-DKD).

We identified a biaryl sulfonamide compound (**1**) in a high-throughput screening (HTS) campaign using an MR binding assay. Subsequent testing in a functional assay demonstrated that the compound was a full MR antagonist.

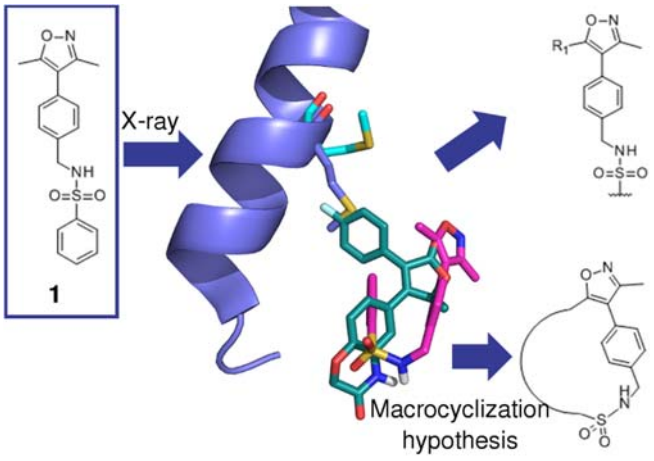

Figure 1. HTS hit (**1**, magenta) and the design idea to expand the biaryl sulfonamides towards the pocket that can be created by movement of the Met852 side chain, as illustrated in the overlay of two complex structures (slate blue: Met852 in HTS hit structure or cyan: Met852 in 3WFG[6]). This pocket accommodates a phenyl substituent of the benzoxazinone ligand (turquoise) in the complex structure by Hasui et al.[6] Lower right displays the design idea to cyclize compound **1** based on the U-shaped binding conformation.

However, this class of ligands have reported activity for several oxosteroid receptors.[13-16] By combining SAR exploration and X-ray structure determination we exploited differences in the ligand binding pockets to improve selectivity towards MR. In addition, careful analysis of the compound binding pose inspired the design of the first macrocyclic oxosteroid receptor antagonist. Finally, using a nuclear translocation assay we discovered that these compounds antagonize MR by blocking aldosterone-mediated receptor translocation into the nucleus. The distinct profile of these compounds may lead to them finding utility as tools to clarify genomic versus non-genomic MR effects.[17]

Results and Discussion

Hit identification

Compound **1** (Figure 1) was identified as an MR ligand in an HTS campaign using a scintillation proximity assay (SPA) with tritiated aldosterone. Single concentration response data of MR binding was followed up in ten point concentration response to confirm binding affinity. Functional activity as an MR antagonist was determined using a reporter gene assay with a GAL4 DNA binding domain (DBD)-MR ligand binding domain (LBD) fusion protein as secondary orthogonal assay.[18] The HTS hit (**1**) bound to MR with an affinity of pK_i=6.6 and had a moderate lipophilic ligand efficiency (LLE=pK_i-log$D_{7.4}$) of 3.4 (Table 1). The functional activity of pIC_{50}=5.9 in the reporter gene assay was in a similar range as for eplerenone (pIC_{50}=6.1, Table 1). However compound **1** displayed a poor selectivity profile with a higher binding affinity to both PR (pK_i=6.9) and GR (pK_i=7.2, Table 2). These results are in agreement with previous published data of this structure class as MR, GR and PR ligands.[13-16]

To build a molecular understanding of how the biaryl sulfonamides drive their functional response and how to optimize both potency and selectivity further, we determined the X-ray structure of the MR LBD in complex with compound **1** (Figure 2A, Table 3). The structure revealed that the isoxazole binds near the polar gatekeeper residues Arg817 and Gln776. At the other end of the ligand binding pocket, compound **1** interacts directly with OD1[1] of Asn770 through a hydrogen bond with the sulfonamide NH. In addition, one of the ligand's sulfonamide oxygen atoms interacts indirectly with both Asn770 ND2[1] and Thr945 via a water molecule. Polar interactions with Asn770 are a key motif among many MR antagonists and computational investigations[20] of the effect on binding affinity by different hydrogen-bonding core fragments has been performed. Beyond the sulfonamide, compound **1** folds back upon itself to form an intramolecular packing interaction between the two phenyl moieties.

To explore the structural drivers of the functional profile of compound **1**, we superimposed this structure onto the structure of MR in complex with aldosterone[19] (Figure 2B). This comparison highlights that in contrast to the isoxazole of compound **1**, the 3-keto moiety of aldosterone is within direct hydrogen bonding distance to both Arg817 and Gln776 (3.1 Å and 2.9 Å, respectively). In addition, in the aldosterone complex structure, the water-mediated contacts to ND2 of Asn770 and to Thr945 by compound **1** are replaced by direct contacts through the C19 hydroxyl group of aldosterone. As such, compound **1** appears to have weaker interactions to both the gatekeeper residues in helices three and five and to Asn770 in helix three, both of which are important functional triggers for receptor activation.[19,21]

Looking across the steroid receptor family, the structure of compound **1** superimposes well on the structure of closely related isoxazole compound (**2a**) in PR (Figure 2C). Interestingly, **2a** is a partial agonist at PR,[14] which emphasizes how small changes in amino acid sequence lead to fundamental differences in the functional response of closely related receptors to a given ligand. A key distinction between the two receptors is that Ser810 in MR is replaced by a methionine (Met759) in PR. This change increases the interaction surface available between helices three and five in PR, and which is a strong agonist driver across the steroid receptor family.[22] As such, the serine to methionine change can potentially explain why an MR antagonist can be a PR partial agonist. Indeed, the naturally occurring human MR Ser810Leu mutation converts progesterone from a partial antagonist to a full agonist at MR and as a result this mutation exacerbates hypertension in pregnant women.[23]

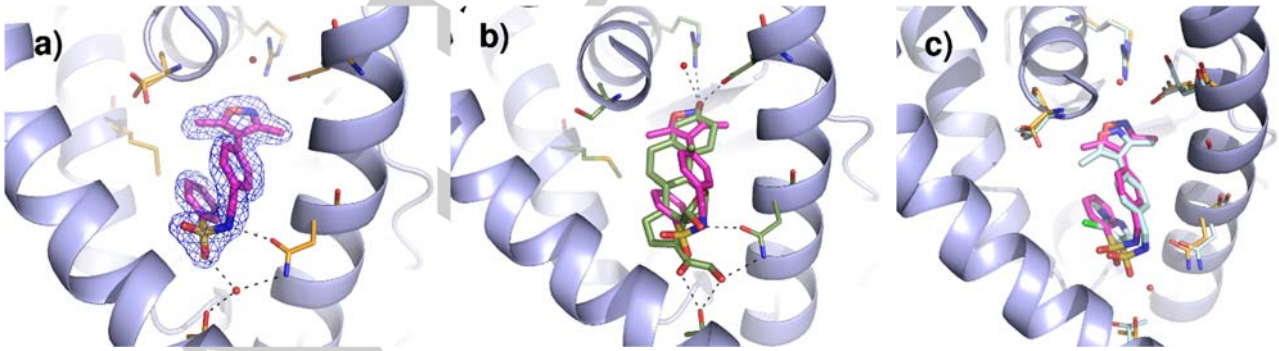

Figure 2. The structure of MR LBD (blue) in complex with compound **1** (magenta). Selected amino acid side chains are shown in orange and putative hydrogen bonds are shown as dotted lines. A) Refined 2mFo-DFc electron density. Ser811 is observed in three distinct conformations. B) Compound **1** superimposed on the structure of MR LBD (amino acid side chains in light green) in complex with aldosterone[19] (light green). C) Compound **1** superimposed on the structure of PR[14] (amino acid side chains in light blue) in complex with isoxazole **2a** (light blue).

[1] Atom names are assigned according to PDB convention.

Table 1. Binding affinity, functional activity and LLE of the profiled MR antagonists.

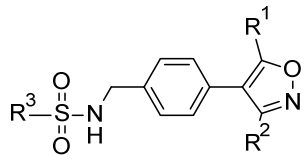

Compound	R^1	R^2	R^3	pIC_{50} RepG hMR[a]	pK_i hMR[b]	$LogD_{7.4}$	LLE[c]
1	CH_3	CH_3	phenyl	5.9 (122%)	6.6±0.04	3.2	3.4
Eplerenone	-	-	-	6.1±0.1 (107%)	6.9±0.1	0.8	6.1
2a[14]	CH_3	CH_3	5-chloro-1,3-dimethyl-pyrazol-4-yl	6.9±0.3 (110%)	7.7±0.1	2.5	5.1
2b	CH_3	CH_3	1-methyl-cyclopropyl	5.9±0.1 (96%)	6.7±0.1	2.5	4.1
2c[13]	CH_3	CH_3	3,5-dimethyl-isoxazol-4-yl	6.7±0.2 (91%)	7.5±0.04[d]	2.8	4.7
8a	H	H	5-chloro-1,3-dimethyl-pyrazol-4-yl	<5.0	5.5±0.1	-	-
13a	CN	CH_3	5-chloro-1,3-dimethyl-pyrazol-4-yl	6.2±0.3 (107%)	7.4±0.2	2.6	4.9
13b	CN	CH_3	1-(difluoromethyl)-3,5-dimethyl-1*H*-pyrazol-4-yl	6.8±0.2 (110%)	7.9±0.2	2.9	5.0
19a	CH_3	CN	5-chloro-1,3-dimethyl-pyrazol-4-yl	6.0±0.1 (107%)[d]	7.0±0.1	2.6	4.4
19b	CH_3	CN	1-(difluoromethyl)-3,5-dimethyl-1*H*-pyrazol-4-yl	6.6±0.2 (109%)	7.3±0.4	3.0	4.2
25a	3-chloro-phenoxymethyl	CH_3	1-methyl-cyclopropyl	6.1±0.1 (116%)	7.5±0.3	>2.9	<4.6
25b	phenoxymethyl	CH_3	1-methyl-cyclopropyl	6.7±0.1 (118%)	7.8±0.3	>3.0	<4.8
25c	3,5-difluoro-phenoxymethyl	CH_3	1-methyl-cyclopropyl	6.7±0.1 (104%)	8.2±0.1	3.8	4.4
25d	2,3-difluoro-phenoxymethyl	CH_3	1-methyl-cyclopropyl	6.3±0.1 (119%)	7.8±0.3[d]	3.8	4.0
25e	4-methyl-phenoxymethyl	CH_3	1-methyl-cyclopropyl	6.5±0.2 (109%)	7.7±0.3[d]	>3.9	<3.8
25f	4-chloro-3-fluoro-phenoxymethyl	CH_3	1-methyl-cyclopropyl	6.5±0.1 (120%)	7.2±0.2	-	-
25g	3-fluoro-5-methyl-phenoxymethyl	CH_3	1-methyl-cyclopropyl	6.3±0.1 (127%)	7.3±0.1	>3.5	<3.8
25h	2-fluoro-5-methyl-phenoxymethyl	CH_3	1-methyl-cyclopropyl	6.3±0.1 (114%)	7.2±0.2[d]	>3.9	<3.3
25i	3-methoxy-phenoxymethyl	CH_3	1-methyl-cyclopropyl	6.7±0.1 (108%)	7.2±0.2	3.8	3.5
25j	2-naphthyloxymethyl	CH_3	1-methyl-cyclopropyl	7.0±0.1 (107%)	7.7±0.1	3.6	4.1
25k	3-acetamidophenoxymethyl	CH_3	1-methyl-cyclopropyl	NA[d,e]	<5.0	3.0	-
25l	4-sulfamoylphenoxymethyl	CH_3	1-methyl-cyclopropyl	NA[d,e]	<5.0	2.2	-
25m	([1-methyl-1*H*-imidazol-2-yl]methoxy)methyl	CH_3	1-methyl-cyclopropyl	NA[d,e]	<5.0	1.5	-
25n	(oxetan-3-yloxy)methyl	CH_3	1-methyl-cyclopropyl	NA[d,e]	<5.0	1.8	-
25o	([1-fluorocyclobutyl]methoxy)-methyl	CH_3	1-methyl-cyclopropyl	6.2±0.1 (104%)	7.0±0.1	2.0	5.0
30	benzyl	CH_3	1-methyl-cyclopropyl	6.4±0.1 (123%)	7.0±0.2	>3	<4.0

[a] Human MR reporter gene pIC_{50} is reported as mean±SD (n ≥ 3, unless noted). Efficacy in percent is reported in parenthesis. [b] Human MR binding affinity pK_i is reported as mean±SD (n ≥ 3, unless noted). [c] LLE=pK_i-$logD_{7.4}$, [d] n=2, [e] NA=not active

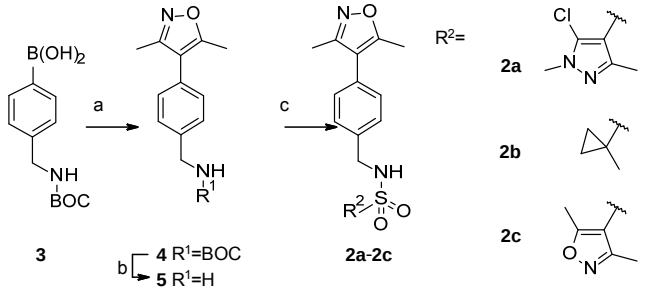

Scheme 1. Synthesis varying the sulfonamide substituent. a) 4-Bromo-3,5-dimethylisoxazole, PEPPSI-IPr, KOH, 1,4-dioxane, 48 h, 65°C, (67%); b) HCl, MeOH, 48 h, rt, (93%); c) RSO_2Cl, NEt_3, CH_2Cl_2, overnight, rt, (58–64%).

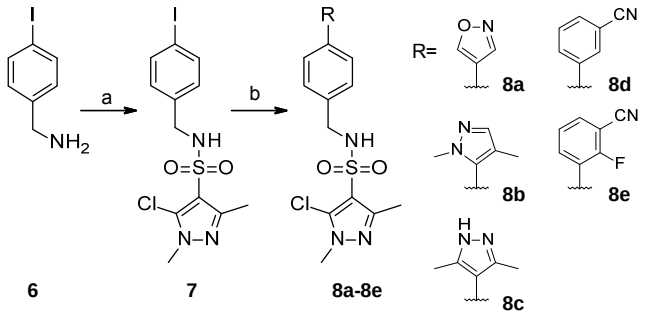

Scheme 2. Synthesis varying the isoxazole part. a) 5-Chloro-1,3-dimethyl-1*H*-pyrazole-4-sulfonyl chloride, Et_3N, CH_2Cl_2, 12 h, 25°C, (92%); $RB(OH)_2$, K_3PO_4, $Pd(dppf)Cl_2$, THF/water, 16 h, 80°C, (10–74%).

Chemistry

The detailed SAR of the sulfonamide aryl group was investigated utilizing parallel chemistry (Scheme 1). Suzuki cross-coupling[24] of the BOC-protected [4-(aminomethyl)phenyl]boronic acid (**3**) and 4-bromo-3,5-dimethylisoxazole with subsequent removal of the BOC-group yielded benzylamine **5**, which was further reacted with selected sulfonyl chlorides to form biaryl sulfonamides **2a**–**2c** in 58–64% yield.

Variation and replacement of the isoxazole moiety was carried out as shown in Scheme 2. Reaction of 4-iodobenzylamine (**6**) with the requisite sulfonyl chloride afforded iodo-substituted sulfonamide **7**, and subsequent Suzuki cross-coupling with selected boronic acids, using $Pd(dppf)Cl_2$ and K_3PO_4 in aqueous THF at 80°C, afforded biaryl compounds **8a**–**8e** (Scheme 2).

The 3- or 5-cyano-substituted isoxazoles **13a**,**b** and **19a**,**b** were synthesized from ethyl acetopyruvate **9** (Scheme 3). For the 5-cyanoisoxazole regioisomers **13a** and **13b**, the reaction of **9** with hydroxylamine[25,26] afforded isoxazole **10**. Ligand-free direct palladium-mediated arylation of **10** with 4-bromobenzonitrile furnished biaryl compound **11**. Conversion of the ester group of **11** to the corresponding primary amide using ammonium hydroxide, followed by catalytic hydrogenation of the nitrile group afforded primary amine **12**. This was reacted with the requisite sulfonyl chloride and the isoxazole 5-carboxamide moiety subsequently converted to the desired nitrile using $POCl_3$ to afford compound **13a**. Compound **13b** was prepared in a similar fashion from compound **12,** with the addition of an alkylation step on the 3,5-dimethylpyrazole intermediate, using sodium chlorodifluoroacetic acid and Cs_2CO_3, to install the desired pyrazole difluoromethyl substituent.

The 3-cyanoisoxazole regioisomers were prepared in a largely similar fashion, but with the functional group conversions in a different order.[27] Reaction of **9** with hydroxylamine at 75°C afforded 3-carboxyisoxazole **14**. Conversion of ester **14** to nitrile **16**, via the corresponding primary amide **15**,[28] was performed before introduction of the 4-aryl moiety. Iodination of **16** with NIS followed by Suzuki cross-coupling with an *N*-BOC-protected boronic acid afforded biaryl **17**. Deprotection under standard conditions followed by reaction with the requisite sulfonyl chloride afforded sulfonamide **19a**. The difluoromethyl moiety of **19b** was installed on the *N*-unsubstituted pyrazole as for **13b**, using chlorodifluoroacetic acid and Cs_2CO_3 in DMF.

Table 2. Binding affinity for GR and PR and selectivity ratio for MR.

Compound	pK_i hGR[a]	pK_i hPR[b]	Selectivity hGR/hMR[c]	Selectivity hPR/hMR[d]
1	7.2±0.3	6.9±0.1	0.29	0.52
Eplerenone	5.5±0.2	4.7±0.2	25	160
2a[14]	7.9±0.3	7.2±0.1	0.52	2.6
2b	6.3±0.2	6.5±0.1	2.1	1.3
2c[13]	8.1±0.3	7.2±0.1	0.26	2.4
13a	7.3±0.1	6.8±0.1	1.5	4.0
13b	7.2±0.1	7.0±0.1	5.1	8.7
19a	7.1±0.1	6.5±0.1	0.89	3.3
19b	6.8±0.4	6.9±0.4	3.1	2.7
25a	6.3±0.1	6.10.3	14	27
25b	6.3±0.3	6.9±0.2	34	7.4
25c	6.3±0.04	6.7±0.2	68	30
25d	6.2±0.1	6.7±0.2	42	14
25e	6.3±0.2	6.9±0.1	23	5.8
25f	6.3±0.2	6.4±0.2	7.4	6.5
25g	6.5±0.1	6.2±0.3	6.7	14
25h	6.3±0.1	6.1±0.3	8.4	14
25i	6.1±0.1	6.1±0.3	13	13
25j	6.8±0.2	6.0±0.2	7.6	41
25o	6.0±0.1	6.3±0.3	10	4.8
39a	6.4±0.2	6.8±0.1	0.59	0.22
39b	6.5±0.1	6.4±0.04	0.43	0.56
44	7.3±0.3	7.5±0.01	1.6	1.0

[a] Human GR binding affinity pK_i is reported as mean±SD (n ≥ 3, unless noted). [b] Human PR binding affinity pK_i is reported as mean±SD (n ≥ 3, unless noted). [c] GR selectivity is reported as the ratio of hGR K_i over hMR K_i. [d] PR selectivity is reported as the ratio of hPR K_i over hMR K_i. [e] n=2

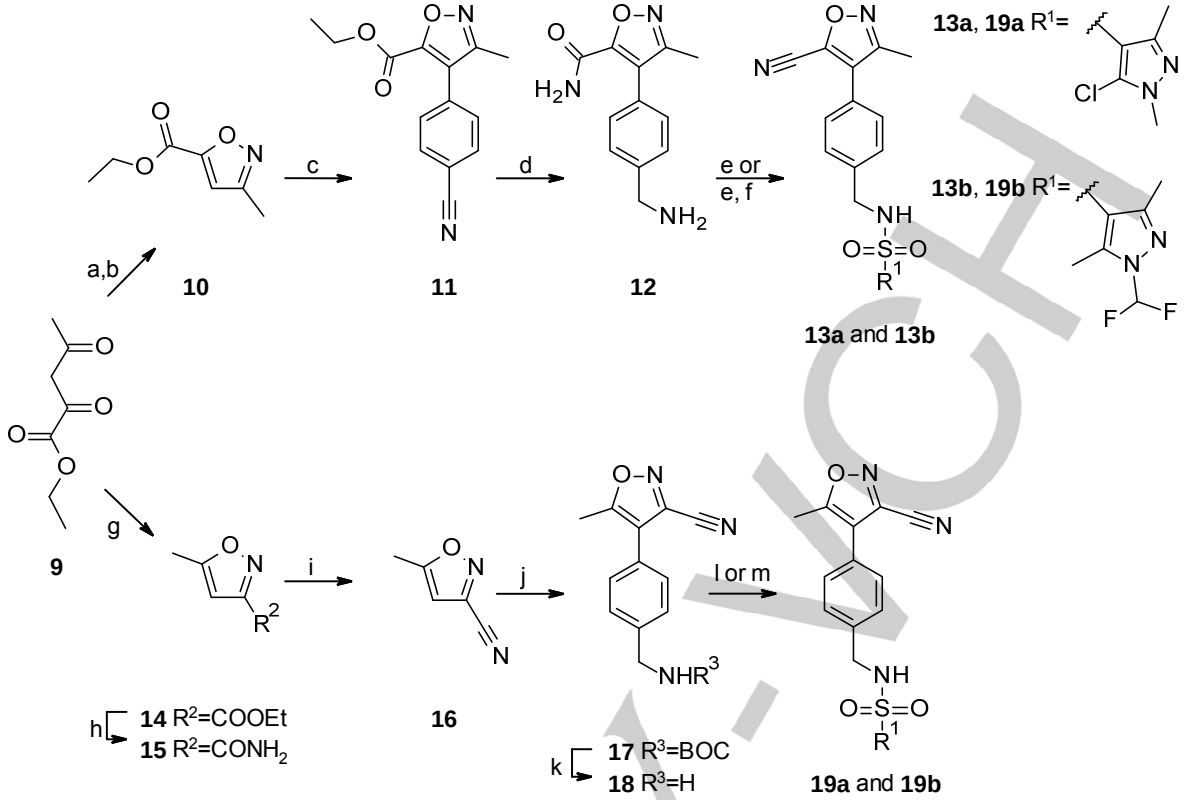

Scheme 3. Synthesis of 3- or 5-cyano substituted isoxazoles. a) NH_2OH, EtOH, 15 min, -5°C, then 3 h, 25°C, (91%); b) H_2SO_4, EtOH, 10 h, 75°C, (74%); c) 4-Bromobenzonitrile, $PdCl_2$, KOAc, DMA, 20 h, 130°C, (37%); d-i) NH_4OH, THF, 15 h, 20°C, d-ii) Pd/C, HCl, MeOH, $H_{2\,(g)}$, 15 h, 25°C, (35% from **11**); e-i) R^1SO_2Cl, Et_3N, CH_2Cl_2, 5–20 h, 25°C e-ii) $POCl_3$, pyridine, –20°C, then 5 h, 25°C, (19%); f) Chlorodifluoroacetic acid sodium salt, Cs_2CO_3, DMF, 5 h, 100°C, (3% from **12**); g) $NH_2OH{\cdot}HCl$, $NaHCO_3$, EtOH, 15 h, 75°C, (85%); h) NH_4OH, THF, 15 h, 25°C, (70%); i) $POCl_3$, pyridine, –20°C, then 15 h, 25°C, (quantitative yield); j-i) NIS, TFA, 3 h, 65°C, j-ii) (4-((BOC-amino)methyl)phenyl)boronic acid, $PdCl_2(PPh_3)_2$, $NaHCO_3$, DMF, 6 h, 95°C, (21% from **16**); k) TFA, CH_2Cl_2, 4 h, 25°C, (73%); l) 5-Chloro-1,3-dimethyl-1*H*-pyrazole-4-sulfonyl chloride, NEt_3, CH_2Cl_2, 20 h, 25°C (23%); m-i) 3,5-Dimethyl-1*H*-pyrazole-4-sulfonyl chloride, NEt_3, CH_2Cl_2, 5 h, 25°C; m-ii) Chlorodifluoroacetic acid sodium salt, Cs_2CO_3, DMF, 5 h, 100°C (17% from **18**).

An ether library exploring the Met852 pocket was designed and synthesized (Scheme 4). The key library intermediate **24** was prepared starting with the reduction of 3-methylisoxazole-5-carboxylic acid (**20**) to the corresponding alcohol **21**. Iodination using NIS yielded aryl iodide **22**. Boronic acid **23** was synthesized from BOC-protected 4-(aminomethyl)phenylboronic acid (**3**). BOC deprotection and reaction with 1-methylcyclopropane-1-sulfonyl chloride gave boronic acid **23**. Suzuki cross-coupling of aryl iodide **22** and boronic acid **23** provided the hydroxymethyl substituted biaryl derivative which was directly mesylated to give **24**. The desired benzylic ethers **25a**–**25o** were synthesized in a parallel fashion from mesylate **24** by nucleophilic substitution with the requisite alcohols.

5-Benzyl-substituted isoxazole (**28**, Scheme 5) was synthesized as previously described.[29,30] Reaction of **28** with NBS afforded bromide **29** which was cross-coupled with BOC-protected 4-(aminomethyl)phenylboronic acid (**3**) using PEPPSI-IPr as catalyst. TFA-mediated BOC removal and reaction of the resulting primary amine with 1-methylcyclopropane-1-sulfonyl chloride afforded sulfonamide **30**.

Macrocycles **39a**, **39b** and **44** were synthesized using a ring-closing metathesis (RCM) strategy as shown in Scheme 6. The synthetic routes to all three macrocycles employed bromoisoxazole **31**[31] as starting point. Palladium-catalyzed borylation of **31** followed by Suzuki cross-coupling with *N*-BOC-4-

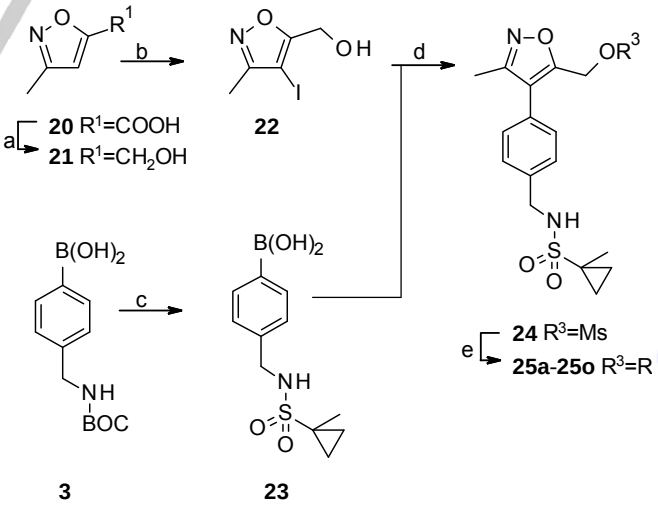

Scheme 4. Synthesis of alcohol library expanding from the isoxazole-5-methyl. a) $BH_3{\cdot}Me_2S$, THF, 30 min, 0°C, then 16 h, rt, (quantitative yield); b) NIS, TFA, 25°C then 30 min, 70°C, (57%); c-i) HCl, 1,4-dioxane, 4 h, 25°C, (91%); c-ii) 1-Methylcyclopropane-1-sulfonyl chloride, NEt_3, CH_2Cl_2, 16 h, 25°C, (80%); d-i) $Pd(PPh_3)_4$, Na_2CO_3, 1,4-dioxane, water, 4 h, 80°C, d-ii) MsCl, NEt_3, CH_2Cl_2, 0°C then 10 min, 25°C, (47%); e) ROH, NaH, DMF, 2 h, 60°C then 16 h, rt, (4–44%).

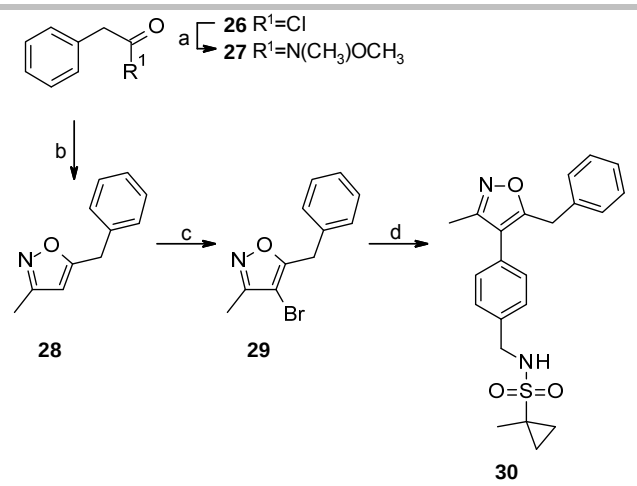

Scheme 5. Synthesis of 5-benzyl substituted oxazole **30**. a) *N*,*O*-Dimethylhydroxylamine*HCl, pyridine, CH_2Cl_2, 0 °C, then, 4 h, rt, (quant.); b) Propan-2-one oxime, BuLi, THF, 0°C, then H_2SO_4, water/THF, 1 h, Δ, (quant.); c) NBS, AcOH, overnight, Δ, (86%); d-i) (4-((BOC-amino)methyl)phenyl)boronic acid, PEPPSI-IPr, KOH, 1,4-dioxane, overnight, 65°C, d-ii) TFA, CH_2Cl_2, overnight, rt; d-iii) 1-Methylcyclopropane-1-sulfonyl chloride, NEt_3, CH_2Cl_2, overnight, rt, (2% from **29**).

bromobenzylamine afforded biaryl compound **32** which upon BOC removal afforded primary amine **33**. This was reacted with 3- or 4-bromobenzenesulfonyl chloride, and subsequent deacetylation using ammonia in methanol afforded sulfonamides **34a** and **34b** respectively. Manganese(IV) oxide mediated oxidation of primary alcohols **34a** and **34b** afforded aldehydes **35a** and **35b**, which were converted to vinylarenes **36a** and **36b** under standard Wittig conditions. Stille coupling of the bromoisoxazole moiety of **36a** and **36b** with allyltributyltin afforded dienes **37a** and **37b**. These dienes then underwent RCM under high dilution conditions at room temperature using second generation Grubbs' catalyst to afford macrocycles **38a** and **38b**. The double bond was reduced by catalytic hydrogenation to obtain the desired macrocycles **39a** and **39b**.

For oxygen-linked macrocycle **44**, deacetylation of **32** followed by Mitsunobu reaction with 3-vinylphenol afforded ether **41**, which afforded benzylamine **42** upon removal of the BOC protecting group. The second alkene moiety was introduced by reaction of amine **42** with allyl sulfonyl chloride, affording diene **43** RCM with second generation Grubbs' catalyst in DCM under high dilution conditions formed the macrocyclic ring, with catalytic hydrogenation of the double bond thus formed affording desired macrocycle **44**.

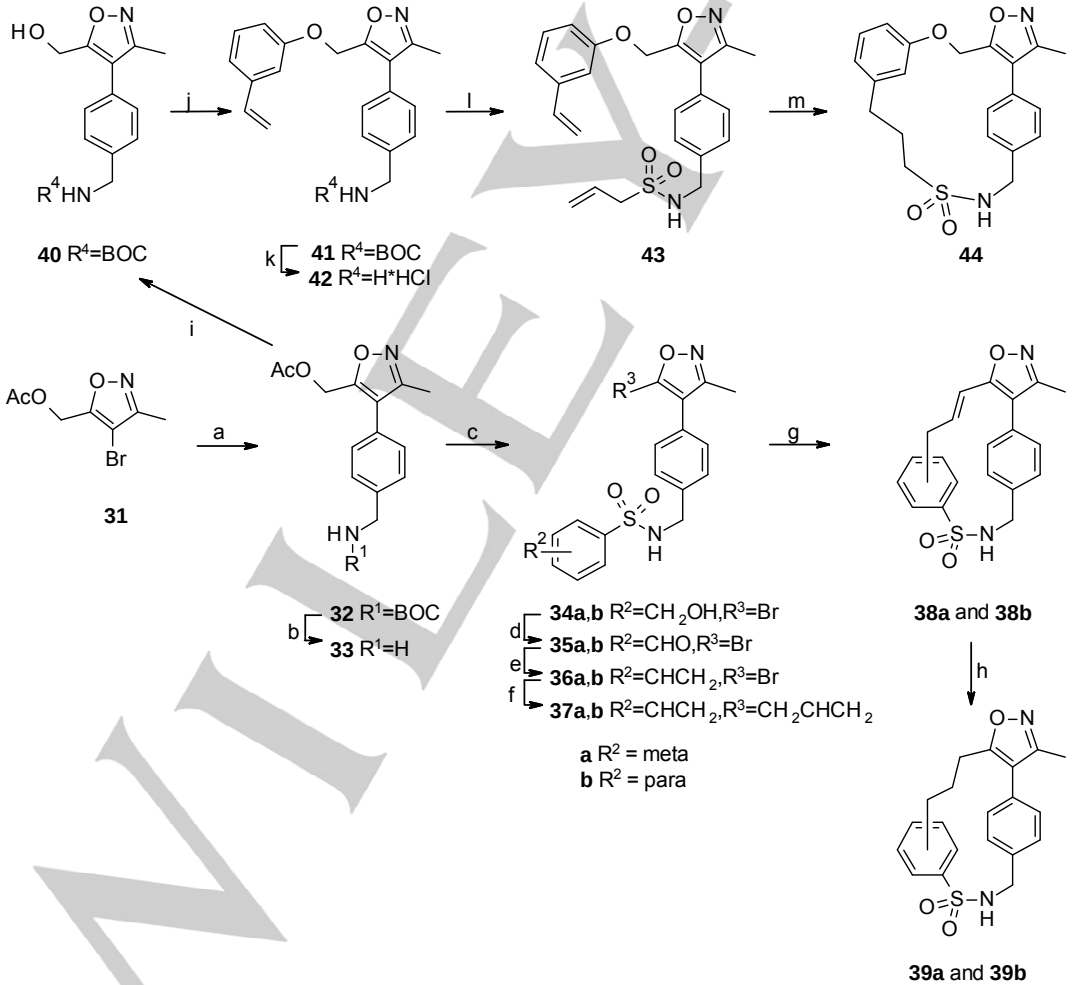

Scheme 6. Synthesis of macrocycles **39a**, **39b** and **44**. a-i) Pinacolborane, $Pd(MeCN)_2Cl_2$, SPhos, toluene, water, 20 h, 90°C; a-ii) *N*-BOC-4-bromobenzylamine, $Pd_2(dba)_3$, Xantphos, $NaHCO_3$, toluene, 12 h, 90°C (46% from **31**), b) 4 M HCl in THF, EtOAc, 12 h, rt, (83%); c-i) 3- or 4-Bromobenzenesulfonyl chloride, pyridine, 12 h, 25°C, c-ii) NH_3, MeOH, 12–20 h, 25°C, (**34a** 51%, **34b** 60% from **33**); d) MnO_2, DCM, 24 h, 25–30°C, (**35a** 85%, **35b** 58%; e) Ph_3PCH_3Br, *t*BuOK, THF, 3–5 h, 0–5°C, (**36a** 41%, **36b** 38%); f) Allyltributyltin, $PdCl_2(dppf)$, DMF, 7–10 h, 90°C, (**37a** 46%, **37b** 22%; g) Grubbs II catalyst, DCM, 6 h, 20–25°C, (**38a** 3%, **38b** 12%); h) 1 atm $H_{2\ (g)}$, Pd/C, EtOAc, 1 h, 20–25°C, (**39a** 58%, **39b** 71%); i) NH_3, MeOH, 20 h, 25°C, (92%); j) 3-Vinylphenol, DEAD, PPh_3, THF, 5 h, 5°C, (52%); k) 4 M HCl in THF, 4 h, 25°C, (73% crude); l) Allylsulfonyl chloride, pyridine, 5 h, 0–25°C, (60%); m) Grubbs II catalyst, DCM, 5 h, 25°C, then 1 atm $H_{2\ (g)}$, Pd/C, EtOAc, 1 h, 30°C, (12%).

Table 3. Data collection and refinement statistics.

Crystal	Compound **1**	Compound **25d**	Compound **44**
Data collection			
PDB ID	5L7E	5L7G	5L7H
Wavelength (Å) (Beamline at ESRF)	0.971 (ID23-1)	0.976 (ID29)	0.972 (ID23-1)
Space group	P212121	P212121	P212121
Cell parameter (Å)	48.62 77.82 78.65	48.63 77.70 78.31	48.67 77.89 78.62
Solvent content (%)	43.31	42.99	43.39
Resolution[a] (Å)	1.86–50.0 (1.86–1.93)	2.01–8.63 (2.01–2.08)	48.67–1.84 (1.84–1.90)
I/Iσ[a]	15.1 (1.8)	11.4 (1.6)	12.2 (1.5)
Completeness[a] (%)	99.0 (91.4)	99.6 (98.6)	100.0 (100.0)
Redundancy[a]	5.7 (2.7)	6.2 (6.3)	6.5 (6.2)
Structure refinement			
Resolution[a] (Å)	41.35–1.86 (1.86–1.94)	41.32–2.01 (2.01–2.12)	42.27–1.84 (1.84–1.92)
Number of reflections used[a]	25453 (2610)	20269 (2869)	26595 (2943)
Fraction of test set for calculating R_{free} (%)	4.67	5.13	5.05
No. of reflections in the test set[a]	1287 (122)	1040 (161)	1343 (153)
R factor: R_{work} /R_{free}[a]	0.180 / 0.197 (0.230 / 0.277)	0.207 / 0.243 (0.229 / 0.257)	0.194 / 0.224 (0.247 / 0.284)
R.m.s.d.			
Bond lengths (Å)	0.010	0.010	0.010
Bond angles (°)	0.96	1.00	0.97
Estimated error (Luzzati plot / DPI by free R[32]) (Å)	0.191 / 0.112	0.293 / 0.163	0.218 / 0.124
B values (mean B value / Wilson plot) (Å^2)	28.47 / 25.52	35.30 / 33.11	32.12 / 38.25
Number of atoms -- final model			
Protein	2142	2136	2181
Water	158	87	181
Ligand	24	31	28

[a] Outer shell values are shown in parenthesis.

Structure–activity relationship

Initial SAR exploration focused on modifications of the sulfonamide substituent and modifications and replacement of the isoxazole moiety. The 1-methyl-cyclopropylsulfonamide substituent of **2b** provided a compound with similar potency and binding affinity to compound **1**, but with a reduced $logD_{7.4}$ resulting in an improved LLE. Compound **2b** possessed similar MR potency to eplerenone (Table 1). Small substituted heterocycles such as in compounds **2a** and **2c** resulted in a 10-fold higher binding affinity and improved functional activity with an increased LLE compared to the HTS hit (**1**), but the selectivity over GR and PR was still poor (Table 2).

The dimethyl substitution pattern on the isoxazole ring was sensitive to modification. Removing the methyl groups on the isoxazole rendered a compound (**8a**) with ~100-fold lower binding affinity than compound **2a** (Table 1). Replacement of the isoxazole ring was also investigated. Replacement of the 3,5-dimethylisoxazol-4-yl moiety with either a 1,4-dimethyl-pyrazol-5-yl (**8b**) or a 3,5-dimethyl-pyrazol-4-yl (**8c**) moiety led to a 4-fold and 10-fold decrease in binding affinity respectively (Table 4). Replacement of the 3,5-dimethylisoxazole by 3-cyanophenyl (**8d**) also led to about a 10-fold loss in binding affinity, in spite of docking studies in crystal structure 5L7E indicating potential interactions between the nitrile group of compound **8d** and gatekeeper residues Gln776 and Arg817. Such an interaction has been observed for ligands at other oxosteroid receptors.[33,34] The introduction of a fluorine substituent *ortho* to the nitrile (**8e**) led to regained binding affinity and functional activity, but at the cost of an increased $logD_{7.4}$ ($logD_{7.4}$=3.1, Table 4) compared to compound **2a** ($logD_{7.4}$=2.5, Table 1).

The preference for the positioning of the isoxazole oxygen and nitrogen in the binding pocket as given in the X-ray structure of compound **1** with MR (Figure 2A) was supported by the regioisomeric pairs **13a**, **19a** and **13b**, **19b**. A 5-cyano-3-methyl-isoxazol-4-yl (**13a** and **13b**) moiety led to 3-4-fold higher binding affinity compared to the 3-cyano-5-methyl-isoxazol-4-yl moiety (**19a** and **19b**). In the complex structure of compound **1**, the 5-position of the isoxazole points towards an area that is occupied by amino acid side chains (of Met852, Ser811 and Leu938) while the 3-position is placed close to the helix three backbone. The 3-cyano regioisomers (**19a** and **19b**) would cause a steric clash with helix three, preventing the preferred orientation of the isoxazole ring, thus disturbing the key polar interactions with the gatekeeper residues Gln776 and Arg817, and resulting in a loss of binding affinity. We propose that the nitrile substituents of **13a**,**b** and **19a**,**b** preferentially occupy the area near Met852, Ser811 and Leu938 on steric grounds, and that the higher binding affinity of the 5-substituted congeners (**13a** and **13b**) reflects the preferred orientation of the isoxazole. Compound **13b** also displayed an improved selectivity over GR and PR (Table 4) compared to the HTS hit (**1**). Docking studies suggest that the nitrile of **13b** interacts directly with MR Ser811, which is an amino acid that differs between MR compared to GR (Ala605) and PR (Val760). In addition, Ser810 in MR is replaced respectively by Met604 and Met759 in GR and PR, leading to an overall more hydrophilic region in the MR receptor compared to that in GR or PR.

Supported by the increased selectivity over GR and PR of compound **13b** we explored if protein-ligand interactions in other areas of the MR LBD could be beneficial to gaining additional oxosteroid receptor selectivity. Using the X-ray structure of MR in complex with compound **1** and a previously published MR structure in complex with a benzoxazinone ligand (PDBcode 3WFG)[6] it was hypothesized that it would be possible to extend the ligand from the isoxazole 5-methyl substituent towards the area around Met852 which is occupied by a phenyl ring of the ligand in 3WFG (Figure 1). We hypothesized that targeting this

Table 4. Binding affinity, functional activity and LLE of the profiled MR antagonists.

	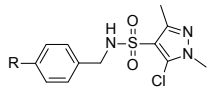 R=	pIC_{50} RepG hMR [a]	pK_i hMR[b]	$LogD_{7.4}$	LLE[c]
8b	1,4-dimethyl-1*H*-pyrazol-5-yl-	6.4±0.2 (108%)	7.0±0.1	2.4	4.6
8c	3,5-dimethyl-1*H*-pyrazol-4-yl-	6.0±0.1 (116%)	6.5±0.1	2.4	4.1
8d	3-cyanophenyl-	6.1±0.1 (102%)	6.6±0.1	3.1	3.5
8e	3-cyano-2-fluorophenyl-	6.6±0.03 (98%)	7.2±0.2	3.1	4.2
39a	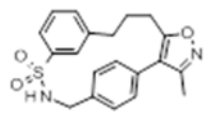	5.6±0.1 (100%)	6.1±0.1	3.3	2.9
39b	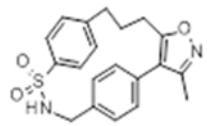	5.7±0.01 (100%)	6.1±0.2	3.2	3.0
44	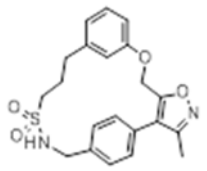	6.6±0.4 (104%)	7.3±0.3	3.0	4.5

[a] Human MR reporter gene pIC_{50} is reported as mean±SD (n ≥ 3, unless noted). Efficacy in percent is reported in parenthesis. [b] Human MR binding affinity pK_i is reported as mean±SD (n ≥ 3, unless noted). [c] LLE=pK_i-$logD_{7.4}$, [d] n=2

pocket could give selectivity for MR, both through direct polar interactions with MR Ser811 and through secondary effects from the required movement of the conserved Met852 side chain in an area where the receptors otherwise differ. In the MR structure in complex with compound **1**, the sidechain of Met852 adopts a similar position as that in the published X-ray structure of MR in complex with aldosterone (PDBcode 2AA2),[19] whereas in public MR antagonist structures (e.g. PDBcode 3WFG), the Met852 sidechain is shown to be moved by the ligand, creating an induced fit pocket that can accommodate phenyl substituents.[6,35,36]

Molecular modeling suggested that a two atom linker extending from the 5-position of the isoxazole would be of suitable length to evaluate this hypothesis and a compound library of ethers was prepared based on compound **2b**. Overall, the ether library (**25a**–**25o**) provided compounds with up to 34-fold improvement in binding affinity (**25c**, pK_i=8.2) and up to 12-fold increase in functional activity (**25j**, pIC_{50}=7.0) (Table 1) compared to matched pair compound **2b**. Although there was a general increase in lipophilicity the improvement in potency was enough to give improvements in LLE. More importantly, an improved selectivity for MR over both GR and PR was observed (Table 2) across the library (**25a**–**25j** and **25o**). The best selectivity profile was observed with compound **25c**. The GR/MR binding affinity ratio was improved 234 fold from a ratio of 0.29 for compound **1** to 68 for compound **25c** and **25c** the had a better selectivity ratio over GR compared to eplerenone. The selectivity over PR was improved 58-fold from a PR/MR binding affinity ratio of 0.52 for compound **1** to 30 for **25c**. The overall best selectivity over PR was observed with compound **25j** (Table 2).

The most potent compounds in the library were the benzylic ethers and where the phenyl ring of the benzylic group had smaller substituents, such as halogens, methyl or methoxy. However, larger groups such as 2-naphthyloxymethyl (**25j**) also provided potent compounds (pIC_{50}=7.0). Compounds with polar phenyl substituents such as **25k** or **25l** or with heterocycles such as the imidazol-2-methyleneyl (**25m**) were inactive. Compound **25n** with an oxetane ring instead of the phenyl ring was also inactive, but examples where the phenyl could be replaced by a non-aromatic systems were identified, here exemplified by compound **25o** (pK_i=7.0).

The structure of MR LBD in complex with **25d** verified that the proposed isoxazole orientation of compound **1** was retained (Figure 3). In addition, the structure confirmed our hypothesis that the sidechain of Met852 would move to accommodate the 2,3-difluorophenoxymethyl moiety (Figure 3). Differences between the oxosteroid receptors can be found in residues in contact with the ligand and with Met852 that is required to move to accommodate the phenyl ether substituent, and we believe that this, at least partially, can rationalize the general selectivity increase of the ether linked compounds (**25a**–**25j** and **25o**) over compound **2b**. None of the biaryl sulfonamide compounds reported in Table 2 displayed binding affinity to rat AR.

The binding pose of compound **25d** positions the 5-benzyloxymethyl isoxazole substituent in close spatial proximity to the 1-methyl-cyclopropyl attached to the sulfonamide functional group at the other end of the molecule. Based upon this observation, the possibility to cyclize the compounds was explored (Figure 1). For compound **1**, the U-shaped binding pose (Figure 2A) places the isoxazole 5-methyl carbon atom either 3.7 Å or 4.0 Å distant from the *para* or closest *meta* carbon atom of the sulfonamide phenyl substituent respectively, suggesting that a two atom linker would be needed to complete the macrocycle.

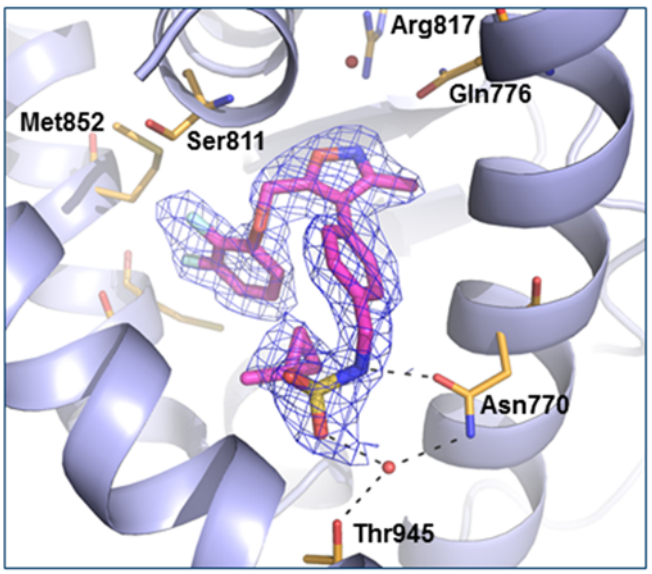

Figure 3. Refined 2mFo-DFc electron density of MR LBD (blue) in complex with compound **25d**. Selected amino acid side chains are shown in orange and putative hydrogen bonds are shown as dotted lines.

Based on compound **1**, two macrocyclic compounds with a three atom linker between either the *meta* or *para* position of the phenyl attached to the sulfonamide and the isoxazole ring were designed to explore conformationally-restrained biaryl sulfonamides. Compared to parent compound **1**, macrocycles **39a** and **39b** both had decreased binding affinity of pK_i=6.1 and functional activity in the reporter gene assay of pIC_{50}=5.6 and 5.7 respectively. This was just on the borderline to be significantly different compared to the linear compound **1** considering the minimum discriminatory difference (MDD) of 0.24 for a compound tested on three different occasions for this assay.

An alternative macrocyclization, based on compound **25b**, of the ether linked phenyl was also explored. In this case macrocyclization from the *meta* position of the ether linked phenyl to the sulfonamide sulfur atom using a three atom linker led to compound **44**. In this case, the binding affinity (pK_i=7.3) and functional activity (pIC_{50}=6.6) was very similar to that of the closest non-cyclized analogue (**25b**, pK_i=7.8, pIC_{50}=6.7). The structure of MR LBD in complex with **44** revealed that despite the conformation constraints imposed by macrocyclization, the interactions to the protein remained intact (Figure 4). A simple conformational search of compound **1** using a molecular mechanics force field and an implicit solvent model suggests that the global minimum and the low energy conformation ensemble are in close proximity to the bound X-ray conformation of **1**. We speculate that the lack of gain in affinity upon macrocyclization is partly due to a limited entropic contribution to binding affinity as a consequence of locking the molecules in their bioactive conformations.

DMPK properties

The HTS hit (**1**) was moderately stable in human hepatocytes (CL_{int}: 7.0 µL/min/10^6 cells), but unstable both in rat hepatocytes (CL_{int}: >300 µL/min/10^6 cells) and in vivo in rats (clearance: 56 mL/min/kg) (Table 5). Compound **1** had moderate kinetic solubility (62 µM) and no glutathione (GSH) conjugates were detected when incubated with human liver microsomes (HLM). In **2b**, where the phenyl sulfonamide substituent of compound **1** was replaced by the saturated 1-methyl cyclopropyl substituent, both solubility (420 µM) and metabolic stability in human hepatocytes (CL_{int}: 1.5 µL/min/10^6 cells) were greatly improved. However, the metabolic stability in rat, both in vitro (CL_{int}: >300 µL/min/10^6 cells) and in vivo (clearance: 56 mL/min/kg), was still low.

Table 5. DMPK data for selected compounds.

	1	**2b**	**25i**	**44**
Solubility (µM)	62	420	0.5	1.5
CL_{int} human/ rat hepatocytes (µL/min/10^6 cells)	7.0 / >300	1.5 / >300	33 / >300	17 / >300
Clearance rat (mL/min/kg)	51	56	52	55
GSH conjugates detected in HLM	No	No	Yes	No
Caco-2 P_{app} (1x10^{-6} cm/s)	70	75	53	96
CYP inhibition[a] (µM)	6.2 (CYP2C19)	3.2 (CYP2C9)	1.4 (CYP2C9)	5.7 (CYP3A4)

[a] Value for the most active CYP given

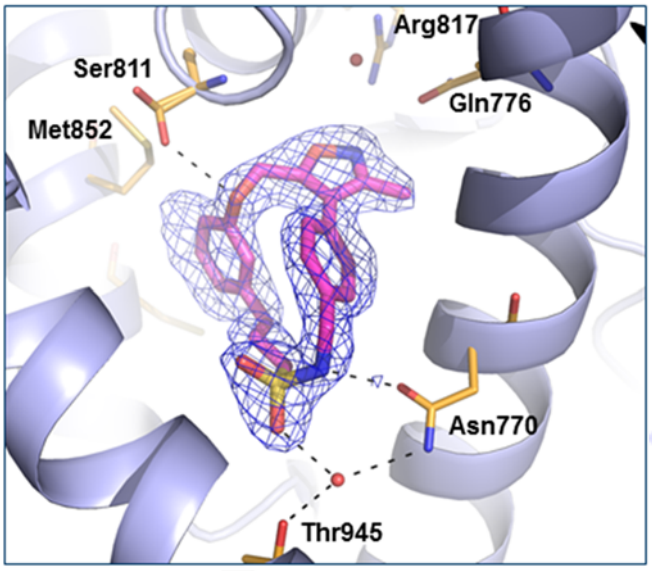

Figure 4. Refined 2mFo-DFc electron density of MR LBD (blue) in complex with compound **44**. Selected amino acid side chains are shown in orange and putative hydrogen bonds are shown as dotted lines. Ser811 is observed in two distinct conformations.

For **25i**, a more potent analogue of **2b** in which the isoxazole 5-methyl was replaced by a 3-methoxy-phenoxymethyl moiety, both solubility (0.5 µM) and metabolic stability in human hepatocytes (CL_{int}: 33 µL/min/10^6 cells) were impaired. Furthermore, significant amounts of GSH conjugates were trapped. The major site of metabolism was identified as the 3-methoxy-phenoxymethyl substituent (data not shown). Also, compound **25i** was unstable in vitro (rat hepatocyte CL_{int} >300 µL/min/10^6 cells) and in vivo in rat (clearance 52 mL/min/kg) For the macrocyclic compound **44**, the issues of poor solubility (1.5 µM) and low in vitro and in vivo metabolic stability (human hepatocyte CL_{int} 17 µL/min/10^6 cells, rat hepatocyte CL_{int} >300 µL/min/10^6 cells, rat clearance: 55 mL/min/kg) were retained For all four compounds the Caco-2 permeability was high (P_{app}: 53–96 1×10^{-6} cm/s).

Biophysical characterization

Nuclear hormone receptor ligands that lack functional agonism at the receptor can be divided into two groups: antagonists, which induce a conformation and an action of the receptor distinct from that of an agonist, or inverse agonists which promote corepressor binding.[37] To further understand the mode of action of the three biaryl sulfonamides (**1**, **25d** and **44**) where the MR-complex structure were solved (Table 3), we studied ligand-dependent MR translocation into the nucleus using EA.hy926 cells, which express MR endogenously. The experiments were performed in the absence or presence of 0.1 nM aldosterone either to study the intrinsic ability of the ligands to translocate MR into the nucleus or their ability to block

Table 6. Residence time and translocation data for hMR.

Compound	k_{off} (s^{-1})	Translocation pEC_{50} (μM)	Translocation block[a] pIC_{50} (μM)
1	0.010	<4.8	6.6 (94%)
25d	0.0048	<5	6.4 (90%)
44	0.0089	<5	7.0 (72%)

[a] Efficacy given in parenthesis

aldosterone-mediated nuclear translocation. All three compounds prevent aldosterone-mediated translocation of MR to the nucleus, which is a potential explanation for their antagonistic behavior in reporter gene assays (Table 6). The three compounds also lack the ability to induce nuclear translocation of MR in the absence of aldosterone.

Compounds **1**, **25d** and **44** were also kinetically characterized using a time-resolved competition SPR assay (Table 6). The 2-fold difference in affinity between **25d** and **44** was also reflected by a 2-fold difference in residence time. However, compound **1** had a similar dissociation rate to **44** despite a 10-fold difference in K_i. This indicates that compound **1** has a slower on rate.

Conclusions

We have identified a series of biaryl sulfonamide MR antagonists that act by blocking aldosterone-induced translocation of MR into the nucleus. Guided by the X-ray structure of the HTS hit (**1**), the compounds were expanded into a cryptic pocket formed by induced fit at the receptor. Targeting this cryptic pocket also gave a general increase in selectivity over GR and PR. We also report the first potent macrocyclic MR antagonist, with a binding affinity pK_i=7.3. We have demonstrated that good solubility, good metabolic stability in human hepatocytes, high permeability and low reactive metabolite formation can be achieved within the compound series. However, the low metabolic stability in rats still needs to be addressed in order to develop a compound suitable for testing in a rat in vivo efficacy model.

Abbreviations

AR, androgen receptor; CIR, confidence interval ratio; CKD, chronic kidney disease; DBD, DNA binding domain; ER, estrogen receptor; GR, glucocorticoid receptor; GSH, glutathione; HLM, human liver microsomes; HTS, high throughput screening; LBD, ligand binding domain; LLE, lipophilic ligand efficiency; MDD, minimum discriminatory difference; MR, mineralocorticoid receptor; PR, progesterone receptor; RCM, ring-closing metathesis; rt, room temperature; SAR, structure–activity relationship; SPA, scintillation proximity assay.

Experimental Section

Chemistry

General Purity of all test compounds was determined by LCMS. All screening compounds had a purity >95%. A complete list of the synthetic procedures and compound characterization is available in the supporting information.

***N*-[4-(3,5-Dimethyl-1,2-oxazol-4-yl)benzyl]benzenesulfonamide (1)** ^{1}H NMR (500 MHz, $CDCl_3$): δ = 2.24 (s, 3H), 2.38 (s, 3H), 4.21 (d, *J* = 6.3 Hz, 2H), 4.77–4.87 (m, 1H), 7.17 (d, *J* = 8.1 Hz, 2H), 7.29 (d, *J* = 8.1 Hz, 2H), 7.50–7.56 (m, 2H), 7.57–7.63 (m, 1H), 7.86–7.93 ppm (m, 2H); HRMS (ESI) *m/z* $[M + H]^+$ calcd for $C_{18}H_{19}N_2O_3S$: 343.1111 found: 343.1118.

***tert*-Butyl *N*-[[4-(3,5-dimethylisoxazol-4-yl)phenyl]methyl]-carbamate (4)** Compound **4** was synthesized from 4-bromo-3,5-dimethylisoxazole (4.0 g, 23 mmol) to afford the title compound (4.6 g, 67%).

[4-(3,5-Dimethylisoxazol-4-yl)phenyl]methanamine hydrochloride (5) Compound **5** was synthesized from *tert*-butyl *N*-[[4-(3,5-dimethylisoxazol-4-yl)phenyl]methyl]-carbamate (**4**, 4.59 g, 15.2 mmol) to afford the title compound (3.4 g, crude yield 93%).

General procedure A for synthesis of *N*-[4-(3,5-dimethyl-1,2-oxazol-4-yl)benzyl]-sulfonamides (2a–2c) [4-(3,5-Dimethylisoxazol-4-yl)phenyl]methanamine hydrochloride (**5**, 70 mg, 0.29 mmol) was dissolved in CH_2Cl_2 (2.5 mL). The appropriate sulfonylchloride (0.32 mmol) and NEt_3 (0.16 mL, 1.2 mmol) were added and the reaction was stirred at rt overnight. The solvent was removed *in vacuo* and the product was purified by preparative HPLC.

5-Chloro-*N*-[4-(3,5-dimethyl-1,2-oxazol-4-yl)benzyl]-1,3-dimethyl-1*H*-pyrazole-4-sulfonamide (2a)[14] Compound **2a** was synthesized according to general procedure A to afford the title compound (62 mg, 58%).

***N*-[4-(3,5-Dimethyl-1,2-oxazol-4-yl)benzyl]-1-methylcyclopropane-sulfonamide (2b)**. Compound **2b** was synthesized according to general procedure A to afford the title compound (60 mg, 64%).

***N*-[4-(3,5-Dimethyl-1,2-oxazol-4-yl)benzyl]-3,5-dimethyl-1,2-oxazole-4-sulfonamide (2c)**[13] Compound **2c** was synthesized according to general procedure A to afford the title compound (63 mg, 59%).

5-Chloro-*N*-[(4-iodophenyl)methyl]-1,3-dimethyl-pyrazole-4-sulfonamide (7) Compound **7** was synthesized from (4-iodophenyl)-methanamine (**6**, 3.9 g, 17 mmol) to afford the title compound (6.0 g, 92%) as an off-white solid.

General procedure B for Suzuki cross-coupling (8a–8e) Into a 40 mL vial, was placed 5-chloro-*N*-[(4-iodophenyl)methyl]-1,3-dimethyl-pyrazole-4-sulfonamide (**7**, 42.6 mg, 0.10 mmol), boronic acid (0.15 mmol), K_3PO_4 (0.20 mmol) and $Pd(dppf)Cl_2$ (5– 10Mol%) in THF:water 4:1 (2 mL). The mixture was stirred at 80°C for 16 h. After cooling to the ambient temperature the crude product was purified by preparative HPLC and lyophilized.

5-Chloro-1,3-dimethyl-*N*-[4-(1,2-oxazol-4-yl)benzyl]-1*H*-pyrazole-4-sulfonamide (8a) Compound **8a** was synthesized according to general procedure B to afford the title compound (14 mg, 39%).

5-Chloro-*N*-[4-(1,4-dimethyl-1*H*-pyrazol-5-yl)benzyl]-1,3-dimethyl-1*H*-pyrazole-4-sulfonamide (8b) Compound **8b** was synthesized according to general procedure B to afford the title compound (29 mg, 74%).

5-Chloro-*N*-[4-(3,5-dimethyl-1*H*-pyrazol-4-yl)benzyl]-1,3-dimethyl-1*H*-pyrazole-4-sulfonamide (8c) Compound **8c** was synthesized according to general procedure B to afford the title compound (4.1 mg, 10%).

5-Chloro-*N*-[(3'-cyanobiphenyl-4-yl)methyl]-1,3-dimethyl-1*H*-pyrazole-4-sulfonamide (8d) Compound **8d** was synthesized according to general procedure B to afford the title compound (17 mg, 43%).

5-Chloro-*N*-[(3'-cyano-2'-fluorobiphenyl-4-yl)methyl]-1,3-dimethyl-1*H*-pyrazole-4-sulfonamide (8e) Compound **8e** was synthesized according to general procedure B to afford the title compound (19 mg, 46%).

Ethyl 3-methylisoxazole-5-carboxylate (10) Ethyl (4*E*)-4-hydroxyimino-2-oxo-pentanoate was prepared as described by Sumimoto[25] (20 g, 91%). Compound **10** was prepared from ethyl (4*E*)-4-hydroxyimino-2-oxo-pentanoate as described by Dannhardt et al.[26] to afford the title compound (4.0 g, 74%).

Ethyl 4-(4-cyanophenyl)-3-methylisoxazole-5-carboxylate (11) Compound **11** was synthesized from ethyl 3-methylisoxazole-5-carboxylate (**10**, 12.5 g, 80.6 mmol) to afford the title compound (6.2 g, 37%) as a pale yellow solid.

4-[4-(Aminomethyl)phenyl]-3-methylisoxazole-5-carboxamide (12) Compound **12** was synthesized from ethyl 4-(4-cyanophenyl)-3-methylisoxazole-5-carboxylate (**11**, 6.5 g, 25 mmol) to afford the title compound (2.0 g, 35% over two steps) as a pink solid.

5-Chloro-*N*-[4-(5-cyano-3-methyl-1,2-oxazol-4-yl)benzyl]-1,3-dimethyl-1*H*-pyrazole-4-sulfonamide (13a) Compound **13a** was synthesized from 4-(4-(aminomethyl)phenyl)-3-methylisoxazole-5-carboxamide (**12**, 300 mg, 1.30 mmol) to afford the title compound (100 mg, 19% over two steps) as a white solid.

***N*-[4-(5-Cyano-3-methyl-1,2-oxazol-4-yl)benzyl]-1-(difluoromethyl)-3,5-dimethyl-1*H*-pyrazole-4-sulfonamide (13b)** Compound **13b** was synthesized 4-(4-(aminomethyl)phenyl)-3-methylisoxazole-5-carboxamide (**12**, 300 mg, 1.30 mmol) to afford the title compound (15 mg, 3% over three steps) as a white solid.

Ethyl 5-methylisoxazole-3-carboxylate (14) was prepared as described by Rao et al.[27] to afford the title compound (25 g, 85%).

5-Methylisoxazole-3-carboxamide (15) was prepared as described by Collins et al.[28] to afford the title compound (1.7 g, 70%).

5-Methylisoxazole-3-carbonitrile (16) was prepared as described by Collins et al.[28] to afford the title compound (9.4 g, quantitative yield).

***tert*-Butyl *N*-[[4-(3-cyano-5-methylisoxazol-4-yl)phenyl]methyl]-carbamate (17)** Compound **17** was synthesized from 5-methylisoxazole-3-carbonitrile (**16**, 10.0 g, 92.5 mmol) to afford the title compound (1.2 g, 21% over two steps) as a brown oil which solidified on standing.

4-[4-(Aminomethyl)phenyl]-5-methylisoxazole-3-carbonitrile (18) Compound **18** was synthesized from *tert*-butyl *N*-[[4-(3-cyano-5-methylisoxazol-4-yl)phenyl]methyl]carbamate (**17**, 1.2 g, 3.8 mmol) to afford the title compound (0.70 g, 73%) as a pale yellow oil which solidified on standing.

5-Chloro-*N*-[4-(3-cyano-5-methyl-1,2-oxazol-4-yl)benzyl]-1,3-dimethyl-1*H*-pyrazole-4-sulfonamide (19a) Compound **19a** was synthesized from 4-(4-(aminomethyl)phenyl)-5-methylisoxazole-3-carbonitrile (**18**, 90 mg, 0.42 mmol) to give the desired product (40 mg, 23%) as a white solid.

***N*-[4-(3-Cyano-5-methyl-1,2-oxazol-4-yl)benzyl]-1-(difluoromethyl)-3,5-dimethyl-1*H*-pyrazole-4-sulfonamide (19b)** Compound **19b** was synthesized from 4-(4-(aminomethyl)phenyl)-5-methylisoxazole-3-carbonitrile (**18**, 150 mg, 0.70 mmol) to afford the title compound (56 mg, 17% over two steps) as a white solid.

(3-Methylisoxazol-5-yl)methanol (21) Compound **21** was synthesized from 3-methylisoxazole-5-carboxylic acid (**20**, 1.0 g, 7.9 mmol) to give the title compound as a colorless syrup (0.89 g, crude yield 100%).

(4-Iodo-3-methylisoxazol-5-yl)methanol (22) Compound **22** was synthesized from (3-Methylisoxazol-5-yl)methanol (**21**, 20.0 g, 159 mmol, 90%) to afford the title compound as a light yellow solid (23 g, 57%).

[4-[[(1-Methylcyclopropyl)sulfonylamino]methyl]phenyl]-boronic acid (23) Compound **23** was synthesized from [4-([[(*tert*-butoxy)carbonyl]amino]methyl)phenyl]boronic acid (**3**, 14 g, 53 mmol, 95%) to afford the title compound as a light yellow solid (14 g, crude yield 80%).

[3-Methyl-4-[4-[[(1-methylcyclopropyl)sulfonylamino]-methyl]-phenyl]isoxazol-5-yl]methyl methanesulfonate (24) Compound **24** was synthesized from (4-iodo-3-methylisoxazol-5-yl)methanol (**22**, 10.4 g, 41.3 mmol) to afford the title compound as a yellow oil (8.0 g, crude yield 47% over two steps).

General procedure C for synthesis of ether linked compounds (25a–25o) Into a 40 mL vial, was placed the appropriate alcohol (0.11 mmol) and NaH (0.11 mmol) in DMF (3 mL). The mixture was stirred at 60°C for 2 h. After cooling to the ambient temperature [3-methyl-4-[4-[[(1-methyl-cyclopropyl)sulfonylamino]-methyl]phenyl]isoxazol-5-yl]methyl methane-sulfonate (**24**, 29 mg, 0.07 mmol) was added into the vial and the mixture was stirred for 16 h at rt and then concentrated *in vacuo*. The crude product was purified by preparative HPLC.

***N*-(4-(5-((3-Chlorophenoxy)methyl)-3-methylisoxazol-4-yl)benzyl)-1-methylcyclopropane-1-sulfonamide (25a).** Compound **25a** was synthesized according to general procedure C to afford the title compound (67 mg, 44%).

1-Methyl-*N*-(4-(3-methyl-5-(phenoxymethyl)isoxazol-4-yl)benzyl)cyclopropane-1-sulfonamide (25b). Compound **25b** was synthesized according to general procedure C to afford the title compound (11 mg, 8%).

***N*-(4-(5-((3,5-Difluorophenoxy)methyl)-3-methylisoxazol-4-yl)benzyl)-1-methylcyclopropane-1-sulfonamide (25c).** Compound **25c** was synthesized according to general procedure C to afford the title compound (2 mg, 4%).

1-Methyl-*N*-[[4-[3-methyl-5-(phenoxymethyl)isoxazol-4-yl]phenyl]methyl]cyclopropanesulfonamide (25d). Compound **25d** was synthesized according to general procedure C to afford the title compound (8.0 mg, 26%).

1-Methyl-*N*-[[4-[3-methyl-5-[(4-methylphenoxy)methyl]isoxazol-4-yl]phenyl]methyl]cyclopropanesulfonamide (25e). Compound **25e** was synthesized according to general procedure C to afford the title compound (5.6 mg, 19%).

***N*-[[4-[5-[(4-Chloro-3-fluoro-phenoxy)methyl]-3-methylisoxazol-4-yl]phenyl]methyl]-1-methyl-cyclopropanesulfonamide (25f)**. Compound **25f** was synthesized according to general procedure C to afford the title compound (0.9 mg, 28%).

***N*-[[4-[5-[(3-Fluoro-5-methyl-phenoxy)methyl]-3-methylisoxazol-4-yl]phenyl]methyl]-1-methyl-cyclopropanesulfonamide (25g).** Compound **25g** was synthesized according to general procedure C to afford the title compound (3.2 mg, 10%).

***N*-[[4-[5-[(2-Fluoro-5-methyl-phenoxy)methyl]-3-methylisoxazol-4-yl]phenyl]methyl]-1-methyl-cyclopropanesulfonamide (25h).** Compound **25h** was synthesized according to general procedure C to afford the title compound (2.8 mg, 9.0%).

***N*-(4-[5-[(3-Methoxyphenoxy)methyl]-3-methyl-1,2-oxazol-4-yl]benzyl)-1-methyl-cyclopropane-sulfonamide (25i)** Compound **25i** was synthesized according to general procedure C to afford the title compound (9.2 mg, 34%).

1-Methyl-*N*-[[4-[3-methyl-5-(2-naphthyloxymethyl)isoxazol-4-yl]phenyl]methyl]cyclopropanesulfonamide (25j). Compound **25j** was synthesized according to general procedure C to afford the title compound (5.1 mg, 16%).

***N*-[3-({3-Methyl-4-[4-({[(1-methylcyclopropyl)sulfonyl]-amino}methyl)phenyl]-1,2-oxazol-5-yl}methoxy)phenyl]acetamide (25k)** Compound **25k** was synthesized according to general procedure C to afford the title compound (3.4 mg, 7%).

4-({3-Methyl-4-[4-({[(1-methylcyclopropyl)sulfonyl]-amino}methyl)phenyl]-1,2-oxazol-5-yl}methoxy)benzenesulfonamide (25l) Compound **25l** was synthesized according to general procedure C to afford the title compound (2.9 mg, 5%).

1-Methyl-*N*-[4-(3-methyl-5-{[(1-methyl-1*H*-imidazol-2-yl)methoxy]methyl}-1,2-oxazol-4-yl)benzyl]cyclopropane-sulfonamide (25m) Compound **25m** was synthesized according to general procedure C to afford the title compound (8.9 mg, 19%).

1-Methyl-*N*-(4-{3-methyl-5-[(oxetan-3-yloxy)methyl]-1,2-oxazol-4-yl}benzyl)cyclopropanesulfonamide (25n) Compound **25n** was synthesized according to general procedure C to afford the title compound (9.8 mg, 23%).

***N*-[4-(5-{[(1-Fluorocyclobutyl)methoxy]methyl}-3-methyl-1,2-oxazol-4-yl)benzyl]-1-methylcyclopropanesulfonamide (25o)** Compound **25o** was synthesized according to general procedure C to afford the title compound (9.1 mg, 20%).

***N*-Methoxy-*N*-methyl-2-phenyl-acetamide (27)** was prepared as described by Rudzinski et al.[29] to afford the title compound (664 mg, quantitative yield).

5-Benzyl-3-methylisoxazole (28) was prepared as described by Nitz et al.[30] to afford the title compound (105 mg, quantitative yield).

5-Benzyl-4-bromo-3-methylisoxazole (29) Compound **29** was synthesized from 5-Benzyl-3-methylisoxazole (**28**, 0.105 g, 0.61 mmol) to afford crude product (131 mg, crude yield 86%) which was directly used in next synthesis step.

***N*-[4-(5-Benzyl-3-methyl-1,2-oxazol-4-yl)benzyl]-1-methylcyclo-propanesulfonamide (30)** Compound **30** was synthesized from 5-Benzyl-4-bromo-3-methylisoxazole (**29**, 0.131 g, 0.52 mmol) to afford the title compound (4.9 mg, 2% over three steps).

***tert*-Butyl *N*-[(4-bromophenyl)methyl]carbamate (45)** was prepared as described by Tashima et al.[38] to afford the title compound (25 g, 81%).

(3-Methylisoxazol-5-yl)methyl acetate (46) was prepared as described by Gehling et al.[31] to afford the title compound as a yellow oil (8.0 g, 51%).

(4-Bromo-3-methylisoxazol-5-yl)methyl acetate (31) was prepared as described by Gehling et al.[31] to afford the title compound as a yellow oil (15.0 g, 66%).

[4-[4-[(*tert*-Butoxycarbonylamino)methyl]phenyl]-3-methylisoxazol-5-yl]methyl acetate (32) Compound **32** was synthesized from (4-bromo-3-methylisoxazol-5-yl)methyl acetate (**31**, 10.0 g, 42.7 mmol) to afford the title compound as a yellow oil (7.0 g, 46% over two steps).

[4-[4-(Aminomethyl)phenyl]-3-methylisoxazol-5-yl]methyl acetate (33) Compound **33** was synthesized from (4-(4-((*tert*-butoxycarbonylamino)methyl)phenyl)-3-methylisoxazol-5-yl)methyl acetate (**32**, 10.0 g, 27.8 mmol) to afford the title compound as a brown oil (6.0 g, crude yield 83%).

3-Bromo-*N*-[[4-[5-(hydroxymethyl)-3-methylisoxazol-4-yl]phenyl]-methyl]benzenesulfonamide (34a) Compound **34a** was synthesized from [4-[4-(aminomethyl)phenyl]-3-methylisoxazol-5-yl]methyl acetate (**33**, 1.5 g, 5.8 mmol) to afford the title compound as a yellow oil (1.3 g, 51% over two steps).

3-Bromo-*N*-[[4-(5-formyl-3-methylisoxazol-4-yl)phenyl]methyl]-benzenesulfonamide (35a) Compound **35a** was synthesized from 3-bromo-*N*-[[4-[5-(hydroxymethyl)-3-methylisoxazol-4-yl]phenyl]methyl]-benzenesulfonamide (**34a**, 1.3 g, 3.0 mmol) to afford the title compound as a yellow oil (1.1 g, 85%).

3-Bromo-*N*-[[4-(3-methyl-5-vinyl-isoxazol-4-yl)phenyl]methyl]benzenesulfonamide (36a) Compound **36a** was synthesized from 3-bromo-*N*-[[4-(5-formyl-3-methylisoxazol-4-yl)phenyl]methyl]benzene-sulfonamide (**35a**, 1.1 g, 2.5 mmol) to afford the title compound as a yellow solid (0.45 g, 41%).

3-Allyl-*N*-[[4-(3-methyl-5-vinyl-isoxazol-4-yl)phenyl]methyl]benzene-sulfonamide (37a) Compound **37a** was synthesized from 3-bromo-*N*-[[4-(3-methyl-5-vinyl-isoxazol-4-yl)phenyl]-methyl]benzenesulfonamide (**36a**, 0.45 g, 1.0 mmol) to afford the title compound as a white solid (0.19 g, 46%).

(17*Z*)-3-Methyl-8,16-dihydro-9*H*-4,7-etheno-11,15-(metheno)[1,2]oxazolo[4,5-*h*][1,2]thiazacycloheptadecine 10,10-dioxide (38a) Compound **38a** was synthesized from 3-allyl-*N*-[[4-(3-methyl-5-vinyl-isoxazol-4-yl)phenyl]methyl]-benzenesulfonamide (**37a**, 1.1 g, 2.8 mmol) to afford the title compound as a white solid (0.03 g, 3%).

3-Methyl-8,16,17,18-tetrahydro-9*H*-4,7-etheno-11,15-(metheno)[1,2]-oxazolo[4,5-*h*][1,2]thiazacycloheptadecine 10,10-dioxide (39a) Compound **39a** was synthesized from (17*Z*)-3-methyl-8,16-dihydro-9*H*-4,7-etheno-11,15-(metheno)[1,2]oxazolo[4,5-*h*][1,2]thiazacycloheptadecine 10,10-dioxide (**38a**, 19 mg, 0.05 mmol) to afford the title compound as a white solid (11 mg, 58%).

4-Bromo-*N*-[[4-[5-(hydroxymethyl)-3-methylisoxazol-4-yl]phenyl]-methyl]benzenesulfonamide (34b) Compound **34b** was synthesized from [4-[4-(aminomethyl)phenyl]-3-methylisoxazol-5-yl]methyl acetate (**33**, 6.0 g, 23 mmol) to afford the title compound as a red oil (6.0 g, 60%).

4-Bromo-*N*-(4-(5-formyl-3-methylisoxazol-4-yl)benzyl)benzene-sulfonamide (35b) Compound **35b** was synthesized from 4-bromo-*N*-[[4-[5-(hydroxymethyl)-3-methylisoxazol-4-yl]phenyl]methyl]benzenesulfonamide (**34b**, 2.6 g, 6.0 mmol) to give the title compound as a yellow oil in (1.5 g, 58%).

4-Bromo-*N*-[[4-(3-methyl-5-vinylisoxazol-4-yl)phenyl]methyl]-benzenesulfonamide (36b) Compound **36b** was synthesized from 4-bromo-*N*-(4-(5-formyl-3-methylisoxazol-4-yl)-benzyl)benzene-sulfonamide (**35b**, 4.0 g, 9.2 mmol) to afford the title compound as a colorless oil (1.5 g, 38%).

4-Allyl-*N*-[[4-(3-methyl-5-vinyl-isoxazol-4-yl)phenyl]methyl]benzene-sulfonamide (37b) Compound **37b** was synthesized from 4-bromo-*N*-[[4-

(3-methyl-5-vinylisoxazol-4-yl)phenyl]methyl]benzenesulfonamide (**36b**, 1.5 g, 3.5 mmol) to afford the title compound as a brown solid (0.30 g, 22%).

3-Methyl-8,15-dihydro-9*H*-4,7:11,14-dietheno[1,2]oxazolo[4,5-*h*][1,2]-thiazacyclohexadecine 10,10-dioxide (38b) Compound **38b** was synthesized from 4-allyl-*N*-[[4-(3-methyl-5-vinyl-isoxazol-4-yl)phenyl]methyl]benzenesulfonamide (**37b**, 450 mg, 1.14 mmol) to afford the title compound as a white solid (50 mg, 12%).

3-Methyl-8,15,16,17-tetrahydro-9*H*-4,7:11,14-dietheno[1,2]oxazolo-[4,5-*h*][1,2]thiazacyclohexadecine 10,10-dioxide (39b) Compound **39b** was synthesized from 3-methyl-8,15-dihydro-9*H*-4,7:11,14-dietheno[1,2]oxazolo[4,5-*h*][1,2]thiazacyclo-hexadecine 10,10-dioxide (**38b**, 28 mg, 0.08 mmol) to afford the title compound as a white solid (20.0 mg, 71.0%).

***tert*-Butyl *N*-[[4-[5-(hydroxymethyl)-3-methylisoxazol-4-yl]phenyl]-methyl]carbamate (40)** Compound **40** was synthesized from [4-[4-[(*tert*-butoxycarbonylamino)methyl]phenyl]-3-methylisoxazol-5-yl]methyl acetate (**32**, 8.0 g, 22 mmol) to afford the title compound as a yellow solid (6.5 g, 92%).

***tert*-Butyl *N*-[[4-[3-methyl-5-[(3-vinylphenoxy)methyl]-isoxazol-4-yl]-phenyl]methyl]carbamate (41)** Compound **41** was synthesized from *tert*-butyl *N*-[[4-[5-(hydroxymethyl)-3-methylisoxazol-4-yl]phenyl]methyl]-carbamate (**40**, 6.50 g, 20.4 mmol) to afford the title compound as a grey solid (4.5 g, 52%).

[4-[3-Methyl-5-[(3-vinylphenoxy)methyl]isoxazol-4-yl]phenyl]methan-amine (42) Compound **42** was synthesized from *tert*-butyl *N*-[[4-[3-methyl-5-[(3-vinylphenoxy)methyl]isoxazol-4-yl]phenyl]methyl]carbamate (**41**, 4.50 g, 10.7 mmol) to afford the title compound as a yellow solid (2.5 g, crude yield 73%).

***N*-[[4-[3-Methyl-5-[(3-vinylphenoxy)methyl]isoxazol-4-yl]phenyl]-methyl]prop-2-ene-1-sulfonamide (43)** Compound **43** was synthesized from [4-[3-methyl-5-[(3-vinylphenoxy)-methyl]isoxazol-4-yl]phenyl]-methanamine (**42**, 2.5 g, 7.8 mmol) to afford the title compound as a yellow solid (2.0 g, 60%).

3-Methyl-8,12,13,20-tetrahydro-9*H*,11*H*-4,7-etheno-14,18-(metheno)[1,2]oxazolo[4,5-*q*][1,10,11]oxathiazacyclononadecine 10,10-dioxide (44) Compound **44** was synthesized from *N*-[[4-[3-methyl-5-[(3-vinylphenoxy)methyl]isoxazol-4-yl]phenyl]methyl]prop-2-ene-1-sulfonamide (**43**, 0.50 g, 1.2 mmol) to afford the title compound as a white solid (60 mg, 12% over two steps).

Protein purification, crystallography, and biological assays

Mineralocorticoid receptor binding assay A 384-well format scintillation proximity assay (SPA) was used to identify compounds that show binding to the human mineralocorticoid receptor LBD. The immobilization of the fusion protein to the scintillation beads was done via rabbit MBP (maltose-binding protein) antibodies that were captured by the anti-rabbit SPA PVT (Polyvinyltoluene) beads. The inhibition of the scintillation signal by displacement of ^{3}H-aldosterone by test compounds was measured on LEADseeker (GE Healthcare). Assay was run in 384-well, white, medium binding plates (Greiner). Assay buffer contained 10 mM Tris pH 7.5 (Sigma-Aldrich), 0.5 mM EDTA (Sigma-Aldrich), 20 mM sodium molybdate dihydrate (Sigma-Aldrich), 10% Glycerol (KEBO Lab) and 0.1 mM DTT (Sigma-Aldrich). A MR/^{3}H-aldosterone solution was prepared by mixing 7 µg/mL MBP-tagged human mineralocorticoid receptor ligand binding domain (residues 729–984) co-infected with p23 lysate (MBP-MR LBD/p23) with 5 nM ^{3}H-aldosterone (Perkin Elmer). 20 µL of MR/^{3}H-aldosterone solution was added to assay plates with 150 nL test or control compound and incubated for 1 h. 2.5 mg/mL SPA imaging beads (Perkin Elmer) and 2 µg/mL anti-MBP antibody (Abcam ltd.) were mixed in the assay buffer and 20 µL of the mix was added to the assay plates. Plates were incubated for at least 8 h in darkness at rt before read on LEADseeker. Compounds were tested in ten-point concentration response (½ log serial dilution) with 37.5 µM starting concentration. Raw data output was analyzed in Screener software (Genedata AG) and IC_{50} values calculated using a four parameter logistic fit. pIC_{50} was reported as mean with the number of experiments n≥3. Confidence interval ratio (CIR) was 1.5 for the MR binding assay with MDD of 0.26 for compounds tested on three occasions. The 95% confidence interval for the true IC_{50} of the compound is the single calculated value of IC_{50} ×/÷ CIR or on a log scale pIC_{50} ± $\log_{10}$(CIR). Two compounds are considered different if their pIC_{50} differ more than ± MDD (p = 0.05).

Mineralocorticoid receptor reporter gene assay A 384-well UAS-MR-bla HEK293 cell based reporter assay (GeneBLAzer®MR DA, ThermoFisher Scientific) was used to identify compounds showing antagonist activity at the human mineralocorticoid receptor LBD. This nuclear receptor assay uses a beta-lactamase reporter (bla) under transcriptional control of an Upstream Activator Sequence (UAS). The UAS is activated by the GAL4 transcription factor DNA Binding Domain (DBD), which is expressed as a fusion protein with the MR LBD (residues 682–984). Upon ligand binding of an agonist (aldosterone), the GAL4(DBD)-MR(LBD) binds to the UAS, which controls transcription of beta-lactamase. Cryo preserved, stably transfected HEK293 cells were thawed and diluted in assay medium (DMEM (Gibco), 2% charcoal stripped fetal bovine serum (Gibco), 100 µg/mL streptomycin,10 units/mL penicillin, 1 mM sodium pyruvate and 1X non-essential amino acid). The cells were seeded, 25000/well in 30 µL assay medium, in a 384 well black/clear TC-treated plate (Corning) and incubated for 4 h at 37°C, 5% CO_2 and 95% humidity. Compound plate with 0.6 µL test or control compound was prediluted 100 times with assay medium and 4 µL of the diluted compound was transferred to the cell plate. The cell plate was incubated for 30 min prior to addition of 4 µL of aldosterone in a final concentration of 1 nM, followed by incubation (as described above) for 16–24 h. The cells were loaded with 8 µL CCF4, a fluorescent substrate buffer containing two connected fluorophores, coumarin and fluorescein, to assess the beta-lactamase activity. The plate was incubated in darkness for 2 h at rt before fluorescence was measured on PHERAstar FS (BMG Labtech) with optic module (FI 405/530/560). The result was presented as the ratio of coumarin/fluorescein fluorescence intensities. Raw data output was analyzed in Screener software (Genedata AG) and IC_{50} values calculated using a four parameter logistic fit. CIR for the MR reporter gene assay was 1.48, for a compound tested on three occasions and the MDD was 0.24.

Fluorescence polarization (FP) ligand binding assays for AR, GR and PR Competition binding studies were performed using Polarscreen™ AR, GR and PR Competitor Assay kits (Life Technologies). Compounds were tested in 10-point concentration response, ½ log serial dilution, final assay start concentration of 50 µM, in black 384-well low volume Corning plates (NBS surface, U bottom). To assay plates with 50 nL test or control compound, 5 µL of either AR Fluormone RED, GR Fluormone RED or PR Fluormone RED were added, followed by 5 µL AR (Rat LBD), GR (Human full length protein) or PR (Human LBD). Final concentrations in the three different assays were 2 nM AR Fluormone RED/ 120 nM AR, 1 nM GR Fluormone RED/ 1500 nM GR or 2 nM PR Fluormone RED/ 150 nM PR respectively. After a 4 h (AR and GR assays) or 2 h (PR assay) incubation time in darkness at rt, the plates were read on a PHERAstar Plus (BMG Labtech) using a FP optic module (540/590/590). Results, in millipolarization (mP), were analyzed in Screener (Genedata AG) and the IC_{50} values were calculated using a 4 parameter logistic fit. pIC_{50} was reported as mean with the number of experiments n≥3. CIR for AR was 1.44, GR 1.61 and PR 1.58 respectively for compounds tested on three occasions and the MDD for each assay was 0.23 for AR, 0.29 for GR and 0.28 for PR.

Mineralcorticoid receptor translocation assay To study ligand activated MR translocation into the nucleus and the blocking effect on MR translocation, we used EA.hy926 cells (ATCC®CRL-2922). Cells were either treated with compounds for MR translocation assay or compounds in presence of 0.1 nM aldosterone for assay in MR translocation blocking mode. Cryo preserved cells were thawed and washed once with assay medium (DMEM (Gibco) with 10% charcoaled stripped FBS (Gibco)) before seeded, 6000 cells/well in 25 µL assay medium, in 384-well Optilux black/clear plates (Corning). Plates were incubated for 24 h at the same conditions as above. 25 nL compound solution was added to the plates by acoustic dispensing (Echo, Labcyte) with a ½ log serial dilution to give a ten point concentration response curve starting at 10 µM. For the MR blocking mode we used 0.1 nM aldosterone (corresponding to EC_{80} value) as an agonist and 25 nL was added to all compound wells. Plates were incubated for 1 h in 37°C, 10% CO_2 and 95% humidity. Medium was completely removed and cells were fixed with 4% buffered paraformaldehyde (Sigma-Aldrich), 50 µL/well, for 20 min at rt. Plates were washed 3 times with PBS, permeabilised with 0.2% Triton-X100 (Sigma-Aldrich) in PBS, 25 µL/well for 15 min at rt and washed three times with PBS. Blocking solution, containing 5% BSA (Sigma-Aldrich) and 5% normal goat serum (Jackson Immunoresearch) in PBS was added, 15 µL/well for 30 min at rt. Blocking solution was removed and primary antibody rMR 1–18 1D5 (DSHB) added, 1/1500 dilution in 5% BSA/PBS and incubated at 4°C ON. Plates were washed twice with PBS/0.05% TWEEN and twice with PBS, followed by addition of 15 µL of secondary antibody, goat-anti-mouse AF488 (InVitrogen) and stained with Hoechst 33342 (InVitrogen) 10 µg/mL in 5% BSA/PBS for 1 h in rt. Plates were washed twice with PBS/0.05% TWEEN and twice with PBS, left with 50 µL PBS/well and sealed. The plates were imaged on ImageXpress Micro system (MolecularDevices) with a 10X Sfluor objective, taking one site per well. Two wavelengths were measured, DAPI and FITC, using the standard filters. The images were quantified using MetaXpress software (MolecularDevices). The difference in fluorescence intensity between the cytoplasm and the nucleus was used to quantify the nuclear translocation/blocking event. Raw data output was analyzed in Screener software (Genedata AG) and EC_{50}/IC_{50} values were calculated using a 4-parameter logistic fit.

Protein expression, purification and crystallization Expression and purification of MR-LBD (amino acids 735-984) with the mutations C808S, C910S and S810L, an N-terminal, TEV cleavable 6-HN tag, and a C-terminal thrombin cleavable co-activator peptide PQAQQKSLLQQLLTE was performed as described previously.[39] Crystals of MR (residues 735–984) C808S, C910S and S810L co-expressed and purified with **44** were grown by sitting drop vapor diffusion in 0.9 M $(NH_4)_2SO_4$, 0.1 M CHES pH 9.5, and 10% (v/v) of condition G5 of Morpheus® Screen (Molecular Dimensions). The same crystallization conditions were used for MR in complex with compounds **25d** and **1** with the exception that 10% (v/v) of Morpheus® conditions C9 and F12 were added to the well solutions respectively instead of condition G5. The crystals were quickly dipped into well solution supplemented with 18% ethylene glycol before being flash frozen in liquid nitrogen.

X-ray structure solution

Complete data were collected at the European Synchrotron Radiation Facility (ESRF, Grenoble, France) for all the crystals. The data were processed with XDS[40] or MOSFLM.[41,42] The structures of MR complexes were determined by molecular replacement using protein data bank (PDB) entry 4UDA[39] as search model. Programs Autobuster[43] and Coot[44] were used for refinement and model building. The final models had zero outliers in the Ramachandran plot. See Table 3 for details of the data collection and structure refinement. The atomic coordinates and the structure factors of the MR complexes have been deposited in the PDB (www.pdb.org) with ID's 5L7E, 5L7G and 5L7H.

Residence time determination. Residence time measurements of MR with ligands was determined using SPR (Biacore). In brief, MR was dialyzed with compound of interest (50 µM). Directly upon dilution and addition of >100-fold excess of competitor (100 µM Aldosterone), the change in receptor binding to surface-immobilized co-factor peptide (PRGC2 146-166), caused by the ligand-induced change in affinity, was monitored by consecutive injection cycles (typically 6×1 min injections) in SPR. The dissociation rate was determined by exponential fits to the positive change in binding rate as a function of time. 120 nM MR in HBSP(+) buffer (10 mM HEPES, 150 mM NaCl, 0,005% P20, pH 7.4) was used for all measurements. The peptide surface was regenerated with 0.005% SDS after each injection.

Lipophilicity[45] Lipophilicity, measured as the distribution coefficient (logD) between octanol and 10 mM sodium phosphate buffer with pH adjusted to 7.4. For all DMPK assays a more detailed assay description is given in the supporting information.

Solubility[45] This method measures the thermodynamic solubility of research compounds based on a shake-flask approach.[47]

Metabolic stability in human and male Han Wistar rat hepatocytes[48] Hepatocyte metabolic stability was determined in accordance with the method described by Jacobson et al.[49]

Intrinsic permeability across Caco-2 cell monolayers A monolayer of Caco-2 cells was used to study the permeability in the apical to basolateral direction.

In vivo rat PK was assessed as previously described.[48] The studies were approved by the Göteborg Animal Research Ethical Board.

Glutathione trapping[50] Compounds were incubated in human liver microsomes in the presence of the trapping agent glutathione and NADPH at pH 7.4 and 37°C.

CYP inhibition in human liver microsomes The objective of this study is to measure the potential of a compound to inhibit a specific cytochrome P450 enzyme in human liver microsomes (HLM).

Acknowledgements

The authors would like to acknowledge the Separation Science Group at AstraZeneca Gothenburg for help with compound purification and HRMS as well as and Global DMPK for support with DMPK and physicochemical profiling.

Keywords: Drug design • Macrocycles • Nuclear hormone receptor • SBDD • NR3C2

References:

[1] J.T. Moore, J.L. Collins, K.H. Pearce, *Chem. Biol.* **2007**, *3*, 891-932.
[2] B. Pitt, F. Zannad, W.J. Remme, R. Cody, A. Castaigne, A. Perez, J. Palensky, J. Wittes, *N. Engl. J. Med.* **1999**, *341*, 709-717.
[3] B. Pitt, W. Remme, F. Zannad, J. Neaton, F. Martinez, B. Roniker, R. Bittman, S. Hurley, J. Kleiman, M. Gatlin, E. Ambrosioni, J.L. Anderson, E. Apetrei, M. Aschermann, J. Banas, S. Cardoso, A. Caspi, N. Chung, R. Corbalan, H.J. Dargie, et al., *N. Engl. J. Med.* **2003**, *348*, 1309-1321.
[4] X. Jeunemaitre, G. Chatellier, C. Kreft-Jais, A. Charru, C. DeVries, P.F. Plouin, P. Corvol, J. Menard, *Am. J. Cardiol.* **1987**, *60*, 820-825.
[5] G. Colussi, C. Catena, L.A. Sechi, *J. Hypertens.* **2013**, *31*, 3-15.
[6] T. Hasui, T. Ohra, N. Ohyabu, K. Asano, H. Matsui, A. Mizukami, N. Habuka, S. Sogabe, S. Endo, C.S. Siedem, T.P. Tang, C. Gauthier, L.A. De Meese, S.A. Boyd, S. Fukumoto, *Bioorg. Med. Chem.* **2013**, *21*, 5983-5994.

[7] A.H. van den Meiracker, R.G. Baggen, S. Pauli, A. Lindemans, A.G. Vulto, D. Poldermans, F. Boomsma, *J. Hypertens.* **2006**, *24*, 2285-2292.
[8] A. Chrysostomou, E. Pedagogos, L. MacGregor, G.J. Becker, *Clin. J. Am. Soc. Nephrol.* **2006**, *1*, 256-262.
[9] L. Tylicki, P. Rutkowski, M. Renke, W. Larczyński, E. Aleksandrowicz, W. Lysiak-Szydlowska, B. Rutkowski, *Am. J. Kidney Dis.* **2008**, *52*, 486-493.
[10] D.A. Sica, *Heart Failure Rev.* **2005**, *10*, 23-29.
[11] M. Collin, F. Niemann, F. Jaisser, *Expert Opin. Ther. Pat.* **2014**, *24*, 177-183.
[12] L. Bärfacker, A. Kuhl, A. Hillisch, R. Grosser, S. Figueroa-Perez, H. Heckroth, A. Nitsche, J. Ergueden, H. Gielen-Haertwig, K. Schlemmer, J. Mittendorf, H. Paulsen, J. Platzek, P. Kolkhof, *ChemMedChem* **2012**, *7*, 1385-1403.
[13] A.R. Brown, M. Bosies, H. Cameron, J. Clark, A. Cowley, M. Craighead, M.A. Elmore, A. Firth, R. Goodwin, S. Goutcher, E. Grant, M. Grassie, S.J.A. Grove, N.M. Hamilton, H. Hampson, A. Hillier, K. Ho, M. Kiczun, C. Kingsbury, S.G. Kultgen, et al., *Bioorg. Med. Chem. Lett.* **2011**, *21*, 137-140.
[14] S.J. Lusher, H.C.A. Raaijmakers, D. Vu-Pham, K. Dechering, T.W. Lam, A.R. Brown, N.M. Hamilton, O. Nimz, R. Bosch, R. McGuire, A. Oubrie, J. de Vlieg, *J. Biol. Chem.* **2011**, *286*, 35079-35086.
[15] S.J. Lusher, H.C.A. Raaijmakers, D. Vu-Pham, B. Kazemier, R. Bosch, R. McGuire, R. Azevedo, H. Hamersma, K. Dechering, A. Oubrie, M. van Duin, J. de Vlieg, *J. Biol. Chem.* **2012**, *287*, 20333-20343.
[16] K. Futatsugi, D.W. Piotrowski, A. Casimiro-Garcia, S. Robinson, M. Sammons, P.M. Loria, M.E. Banker, D.N. Petersen, N.J. Schmidt, *Bioorg. Med. Chem. Lett.* **2013**, *23*, 6239-6242.
[17] E. Gomez-Sanchez, C. Gomez-Sanchez, *Compr Physiol* **2014**, *4*, 965-94.
[18] S.A. Qureshi, P. Sanders, K. Zeh, M. Whitney, B. Pollok, R. Desai, P. Whitney, M. Robers, S.A. Hayes, *Assay Drug Dev. Technol.* **2003**, *1*, 767-776.
[19] R.K. Bledsoe, K.P. Madauss, J.A. Holt, C.J. Apolito, M.H. Lambert, K.H. Pearce, T.B. Stanley, E.L. Stewart, R.P. Trump, T.M. Willson, S.P. Williams, *J. Biol. Chem.* **2005**, *280*, 31283-31293.
[20] K. Roos, A. Hogner, D. Ogg, M.J. Packer, E. Hansson, K.L. Granberg, E. Evertsson, A. Nordqvist, *J. Comput. Aided Mol. Des.* **2015**, *29*, 1109-1122.
[21] J. Huyet, G.M. Pinon, M.R. Fay, J. Fagart, M. Rafestin-Oblin, *Mol. Pharmacol.* **2007**, *72*, 563-571.
[22] J. Zhang, J. Simisky, F.T.F. Tsai, D.S. Geller, *Proc. Natl. Acad. Sci. U. S. A.* **2005**, *102*, 2707-2712.
[23] D.S. Geller, A. Farhi, N. Pinkerton, M. Fradley, M. Moritz, A. Spitzer, G. Meinke, F.T.F. Tsai, P.B. Sigler, R.P. Lifton, *Science (Washington, D. C.)* **2000**, *289*, 119-123.
[24] M.G. Organ, S. Calimsiz, M. Sayah, K.H. Hoi, A.J. Lough, *Angew. Chem. , Int. Ed.* **2009**, *48*, 2383-2387.
[25] S. Sumimoto, *Kogyo Kagaku Kaishi* **1963**, 1831-1837.
[26] G. Dannhardt, W. Fiefer, G. Lambrecht, S. Laufer, E. Mutschler, J. Schweiger, H.G. Striegel, *Eur. J. Med. Chem.* **1995**, *30*, 839-850.
[27] J.M.R. Rao, N. Arumugam, M.M. Ansari, C. Gudla, S. Pachiyappan, M. Ramalingam, J. George, G.F. Arul, Y.K. Bommegowda, S.K. Angupillai, R. Kottamalai, P. Jidugu, D.S. Rao, *PCT Int. Appl.,* WO2012011125A1, **2012.**
[28] M.R. Collins, V. Natarajan, *PCT Int. Appl.,* WO2006043145A1, **2006.**
[29] D.M. Rudzinski, C.B. Kelly, N.E. Leadbeater, *Chem. Commun. (Cambridge, U. K.)* **2012**, *48*, 9610-9612.
[30] T.J. Nitz, D.L. Volkots, D.J. Aldous, R.C. Oglesby, *J. Org. Chem.* **1994**, *59*, 5828-5832.
[31] V.S. Gehling, M.C. Hewitt, R.G. Vaswani, Y. Leblanc, A. Côté, C.G. Nasveschuk, A.M. Taylor, J. Harmange, J.E. Audia, E. Pardo, S. Joshi, P. Sandy, J.A. Mertz, R.J. Sims, L. Bergeron, B.M. Bryant, S. Bellon, F. Poy, H. Jayaram, R. Sankaranarayanan, et al., *ACS Med. Chem. Lett.* **2013**, *4*, 835-840.
[32] D.W.J. Cruickshank, *Acta Crystallogr. , Sect. D: Biol. Crystallogr.* **1999**, *D55*, 583-601.
[33] S.K. Thompson, D.G. Washburn, J.S. Frazee, K.P. Madauss, T.H. Hoang, L. Lapinski, E.T. Grygielko, L.E. Glace, W. Trizna, S.P. Williams, C. Duraiswami, J.D. Bray, N.J. Laping, *Bioorg. Med. Chem. Lett.* **2009**, *19*, 4777-4780.
[34] Z. Zhang, A.M. Olland, Y. Zhu, J. Cohen, T. Berrodin, S. Chippari, C. Appavu, S. Li, J. Wilhem, R. Chopra, A. Fensome, P. Zhang, J. Wrobel, R.J. Unwalla, C.R. Lyttle, R.C. Winneker, *J. Biol. Chem.* **2005**, *280*, 28468-28475.
[35] T. Hasui, N. Matsunaga, T. Ora, N. Ohyabu, N. Nishigaki, Y. Imura, Y. Igata, H. Matsui, T. Motoyaji, T. Tanaka, N. Habuka, S. Sogabe, M. Ono, C.S. Siedem, T.P. Tang, C. Gauthier, L.A. De Meese, S.A. Boyd, S. Fukumoto *J. Med. Chem.* **2011**, *54*, 8616-8631.
[36] T. Hasui, N. Ohyabu, T. Ohra, K. Fuji, T. Sugimoto, J. Fujimoto, K. Asano, M. Oosawa, S. Shiotani, N. Nishigaki, K. Kusumoto, H. Matsui, A. Mizukami, N. Habuka, S. Sogabe, S. Endo, M. Ono, C.S. Siedem, T.P. Tang, C. Gauthier, et al., *Bioorg. Med. Chem.* **2014**, *22*, 5428-5445.
[37] P. Germain, B. Staels, C. Dacquet, M. Spedding, V. Laudet, *Pharmacol. Rev.* **2006**, *58*, 685-704.
[38] T. Tashima, H. Murata, H. Kodama, *Bioorg. Med. Chem.* **2014**, *22*, 3720-3731.
[39] K. Edman, A. Hosseini, M. Bjursell, A. Aagaard, L. Wissler, A. Gunnarsson, T. Kaminski, C. Köhler, S. Bäckström, T. Jensen, A. Cavallin, U. Karlsson E. Nilsson, D. Lecina, R. Takahashi, C. Grebner, S. Geschwindner, M. Lepistö, A. Hogner, V. Guallar, *Structure* **2015**, *23*, 2280-2290.
[40] W. Kabsch, *Acta Crystallogr. , Sect. D: Biol. Crystallogr.* **2010**, *66*, 125-132.
[41] S. Bailey, *Acta Crystallogr. , Sect. D: Biol. Crystallogr.* **1994**, *D50*, 760-763.
[42] A.G.W. Leslie, H.R. Powell in *Processing diffraction data with mosflm,* (Eds.: Read R.J., Sussman J.L.), Springer Netherlands, Dordrecht, **2007**, pp. 41-51.
[43] G. Bricogne, E. Blanc, M. Brandl, C. Flensburg, P. Keller, W. Paciorek, P. Roversi, O.S. Smart, C. Vonrhein, T.O. Womack, *BUSTER* **2009**, 2.11.1.
[44] P. Emsley, K. Cowtan, *Acta Crystallogr. , Sect. D: Biol. Crystallogr.* **2004**, *D60*, 2126-2132.
[45] S. Winiwarter, B. Middleton, B. Jones, P. Courtney, B. Lindmark, K.M. Page A. Clark, C. Landqvist, *J. Comput. Aided Mol. Des.* **2015**, *29*, 795-807.
[46] M.C. Wenlock, T. Potter, P. Barton, R.P. Austin, *J. Biomol. Screening* **2011**, *16*, 348-355.
[47] H. Wan, A.G. Holmen, *Comb. Chem. High Throughput Screening* **2009**, *12*, 315-329.
[48] M. Geyer, E. Wellner, U. Jurva, S. Saloman, D. Armstrong, R. Tacke, *ChemMedChem* **2015**, *10*, 911-924.
[49] L. Jacobson, B. Middleton, J. Holmgren, S. Eirefelt, M. Fröjd, A. Blomgren, L. Gustavsson, *Assay Drug Dev. Technol.* **2007**, *5*, 403-415.
[50] M. Lemurell, J. Ulander, S. Winiwarter, A. Dahlen, Ö Davidsson, H. Emtenäs, J. Broddefalk, M. Swanson, D. Hovdal, A.T. Plowright, A. Pettersen, M. Ryden-Landergren, J. Barlind, A. Llinas, M. Herslöf, T. Drmota, K. Sigfridsson, S. Moses, C. Whatling, *J. Med. Chem.* **2015**, *58*, 897-911.

10.1002/cmdc.201600529

WILEY-VCH

FULL PAPER

Entry for the Table of Contents

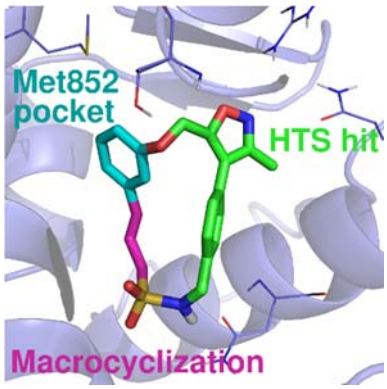

A biarylsulfonamide was identified as a mineralocorticoid receptor antagonist in an HTS campaign. Structure–based drug design was used to improve selectivity over the oxosteroid receptors by exploring an induced fit pocket and expanding the ligands towards an area where the receptors differ from each other. X-ray crystallography confirmed the binding mode and inspired macrocyclization to test conformationally-restrained MR antagonists.